

Linköping Studies in Science and Technology  
Dissertations No 1721

# Variation-Aware System Design Simulation Methodology for Capacitive BCC Transceivers

Muhammad Irfan Kazim



Division of Integrated Circuits and Systems  
Department of Electrical Engineering  
Linköping University  
SE-581 83 Linköping, Sweden  
Linköping 2015

Linköping Studies in Science and Technology  
Dissertations No 1721

Muhammad Irfan Kazim  
`irfan.kazim@isy.liu.se`  
`www.eks.isy.liu.se`  
Division of Integrated Circuits and Systems  
Department of Electrical Engineering  
Linköping University  
SE-581 83 Linköping, Sweden

Copyright © 2015 Muhammad Irfan Kazim, unless otherwise noted.  
All rights reserved.

Muhammad Irfan Kazim  
Variation-Aware System Design Simulation Methodology for Capacitive BCC  
Transceivers  
ISBN 978-91-7685-906-3  
ISSN 0345-7524

Typeset with L<sup>A</sup>T<sub>E</sub>X 2<sub>ε</sub>  
Printed by LiU-Tryck, Linköping, Sweden 2015

*To my loving parents,  
my beloved wife Dr. Saima Nawaz,  
and jewels of my eyes, Maryam and Sarah.*



# Abstract

Capacitive body coupled communication (BCC), frequency range 500 kHz to 15 MHz <sup>1</sup>, is considered an emerging alternate short range wireless technology which can meet the stringent low power consumption ( $< 1$  mW)<sup>2</sup> and low data rate ( $< 100$  kbps)<sup>3</sup> requirements for the next generation of connected devices for applications like internet-of-things (IoT) and wireless sensor network (WSN). But a reliable solution for this mode of communication covering all possible body positions and maximum communication distances around the human body could not be presented so far, despite its inception around 20 years back in 1995. The uncertainties/errors associated with experimental measurement setup create ambiguity about the measured propagation loss or transmission errors. The reason is the usage of either earth grounded lab instruments or the direct coupling of earth ground with transmitter/receiver or the analog front end cut-off frequency limitations in a few MHz region or the balun to provide isolation or the measurements on simplified homogeneous biological phantoms. Another source of ambiguity in the experimental measurements is attributed to the natural variations in human tissue electrophysiological properties from person to person which are also affected by physical factors like age, gender, number of cells at different body locations and humidity. The analytical models presented in the literature are also oversimplified which do not predict the true propagation loss for capacitive BCC channel.

An attempt is being made to understand and demonstrate, qualitatively and quantitatively, the physical phenomenon of signal transmission and propagation characteristics e.g., path loss in complex scenarios for capacitive BCC channel by both the experimental observations/measurements and simulation models in this PhD dissertation. An alternate system design simulation methodology has been proposed which estimates the realistic path loss even for longer communication distances  $> 50$  cm for capacitive BCC channel. The proposed simulation methodology allows to vary human tissue dielectric/thickness properties and easily integrates with the circuit simulators as the output is in the form of S-parameters. The advantage is that the capacitive BCC channel characteristics e.g., signal attenuation as a function of different physical factors could be readily simulated at the circuit level to choose appropriate circuit topology and define suitable system specifications. This simulation methodology is based on full-wave electromagnetic analysis and 3D modeling of human body and environment using their conductivity, permittivity, and tangent loss profile to estimate the realistic propagation loss or path loss due to their combined interaction with the electrode coupler for capacitive BCC channel. This methodology estimates the complex path impedance from transmitter to receiver which is important to determine the matching requirements for maximum power transfer. The simulation methodology also contributes towards better understanding of

---

<sup>1</sup>Optimum frequency in authors opinion as a consequence of PhD research

<sup>2</sup>Ideally speaking power consumption for mobile platforms

<sup>3</sup>Low data rate considered in this thesis

signal propagation through physical channel under the influence of different electrode coupler configurations. The simulation methodology allows to define error bounds for variations in propagation loss due to both numeric uncertainties (boundary conditions, mesh cells) and human body variation uncertainties (dielectric properties, dielectric thicknesses) for varying communication distances and coupler configuration/sizes.

Besides proposing the simulation methodology, the digital baseband and passband communication architectures using discrete electronics components have been experimentally demonstrated in the context of IoT application through capacitive BCC channel for data rates between 1 kbps to 100 kbps under isolated earth ground conditions. The experimental results/observations are supported by the simulation results for different scenarios of capacitive BCC channel.

The experimental and simulation results help in defining suitable system specifications for monolithic integrated circuit design of analog front end (AFE) blocks for capacitive BCC transmitter/receiver in deep submicron CMOS technologies.

# Populärvetenskaplig sammanfattning

Kapacitivt kopplad kommunikation genom kroppen, inom frekvensområdet 100 kHz till 100 MHz, anses vara en alternativ teknik för trådlös kommunikation över korta avstånd. Tekniken kan uppfylla stränga krav på låg effektförbrukning ( $< 1$  mW) och låg datatakt ( $< 100$  kbps). Möjliga applikationer är nästa generations mobila enheter, inom områden som Internet of Things (IoT) och trådlösa sensornätverk.

Trots att forskningen inom området startade 1995 har man hittills inte kunnat presentera en tillförlitlig lösning för detta sätt att kommunicera som täcker alla tänkbara kroppsställningar och maximala kommunikationsavstånd genom den mänskliga kroppen. Osäkerheter/fel i experimentella mätuppställningar skapar ofta oklarhet om de verkliga utbredningsförlusterna och överföringsfelen. Detta på grund av antingen jordkopplade labinstrument eller jordade mottagare/sändare; begränsningar i de analoga gränssnitten; eller användning av baluner som döljer information i mätningar på förenklade, biologiska fantomer. En annan källa till tvetydighet i de experimentella mätningarna beror på variationer i egenskaper hos den mänskliga vävnaden, på grund av exempelvis ålder, kön, hållning och fuktighet. De analytiska modeller som presenterats i litteraturen är också kraftigt förenklade och kan inte användas för att förutsäga den verkliga utbredningsförlusten för en kapacitiv BCC-kanal.

I denna avhandling görs en ansats till att bättre förklara signalöverföring genom en kapacitiv BCC-kanal genom att utnyttja både experimentella observationer och simuleringsmodeller som hittills inte har tydligt framgått.

En alternativ metodik föreslås, där systemsimuleringar används för att uppskatta den realistiska utbredningsförlusten även för längre sträckor ( $> 50$  cm) över en kapacitiv BCC-kanal med isolerad jord. Olika mänskliga vävnadstyper med olika tjocklek och dielektriska egenskaper integreras med kretssimulatorer. Resultatet presenteras i form av S-parametrar. Fördelen med metoden är att de flesta verkliga oönskade effekterna i en BCC-kanal enkelt kan simuleras på kretsnivå för att så kunna välja en lämplig kretstopologi och definiera lämpliga systemspecifikationer.

Denna simuleringsmetodik bygger på full-våg elektromagnetisk analys och 3D-modellering av människokroppen och dess omgivning, genom att använda deras ledningsförmåga och permittivitet för att uppskatta den verkliga utbredningsförlusten på grund av deras kombinerade interaktion med elektrodkopplaren för den kapacitiva BCC-kanalen. Denna metodologi uppskattar den komplexa vägimpedansen från sändare till mottagare, vilket är viktigt för att kunna bestämma matchningskraven för maximal effektöverföring. Metoden bidrar även till bättre förståelse av signalutbredning genom fysiska kanaler under inverkan av olika elektrodkopplingar. Den gör det även möjligt att definiera felintervall för variationer i utbredningsförluster på grund av både numeriska osäkerheter och variationer i den mänskliga kroppen för olika kommunikationsavstånd och kopplare.

Förutom att föreslå denna simuleringsmetodik demonstrerar avhandlingen

kommunikationsarkitekturer för digitala basband och simplex passband, för IoT-användning av kapacitiva BCC-kanaler för datahastigheter mellan 1 kbps och 100 kbps under isolerade jordförhållanden. De experimentella observationer som sågs i labbet stöds av simuleringsresultaten för olika scenarier för den kapacitiva BCC-kanalen.

Dessa resultat bidrar till att definiera systemspecifikationer för en lämplig arkitektur för sändare/mottagare via kapacitiv BCC. Avhandlingen bidrar även till design av integrerade kretsar för analoga gränssnitt till kapacitiva BCC-transceivers i submikrona CMOS-teknologier.

# Acknowledgments

First and foremost, I would like to thank Almighty Allah, the most Gracious and the most Merciful, for giving me physical strength, mental capabilities, healthy heart and mind, supporting parents and family members, guiding teachers, helpful friends and colleagues, useful resources and an enabling environment to carry out this piece of research.

I would like to express my sincere and deepest gratitude towards the following people, without whom this research would have never been possible:

- My PhD advisor and teacher, Dr. J. Jacob Wikner, for his guidance, patience, kindhearted moral and technical support through out these four years of research.
- My head of divisions and teachers, Dr. Oscar Gustafsson and Prof. Atila Alvandpour for encouraging me to pursue the research goals.
- My brief collaboration with Kiran, Bibin and Dilip former graduates from Linköping university and Jan Hederen (Ericsson) who laid down the foundations of BCC research at Linköping university.
- My in-house collaboration with Prakash Harinkumar in the beginning phase of my research in developing an understanding for multistage amplifiers and compensation schemes.
- My collaboration with Ricardo Matias of University of Aveiro, Portugese in the middle phase of my research which helped me the most in redefining the goals of my PhD research.
- My very brief collaboration with Alfredo Pérez Fernández of NTNU, Norway at the ending phase of my research for useful discussions on the simplest daily life applications where capacitive BCC could possibly be used.
- My full time collaboration with my younger brother Dr. Muhamamd Imran Kazim, who did his PhD from Eindhoven University of Technology, Netherlands, who was always there technically and morally when ever I needed him, for helping me in developing an understanding for electromagnetics and its tools for proposing the simulation methodology.
- Among many students which I supervised during Masters thesis, I would specially like to mention Md Hasan Maruf, Koreshi Abdullah and Rahman Ali who initially worked on receiver front end amplifier, transmitter output driver and digital baseband, respectively for BCC.
- Peter Dyreklev (Acreo) project manager for VINNOVA and Anurak Sawatdee (Acreo) for sharing resources in the context of printed electrodes and digital tag.

- Peter Johansson (Forskningsingenjör) for helping me in the labs for conducting BCC experiments.
- My teacher and co-supervisor Prof. Mark Vesterbacka and my other teachers who taught me PhD courses, Assoc Prof. Jerzy Dabrowski, Assoc. Prof. Kent Palmvist, Assoc. Prof Mikael Olofsson, Adjunct Professor Ted Johansson, Prof. Magnus Klofsten and Deyu Tu.
- The former and present colleagues at the Divisions of (former) Electronics Systems and (present) Integrated Circuits and Systems, Department of Electrical Engineering, Linköping University for their help, support and creating a friendly learning environment. I would specially like to express my gratitude to Doctorand Joakim Alvabrant, Doctorand Niklas U Andersson, Doctorand Carl Ingemarsson, Doctorand Petter Källström, Doctorand Vishnu Unnikrishnan, Doctorand Vahid Keshmiri, Doctorand Syed Ahmed Amir, Doctorand Muhammad Fahim ul Haque, Doctorand Syed Asad Alam, Doctorand Muhammad Touqeer Pasha, Doctorand Saima Athar, Dr. Fahad Qazi, Dr. Nadeem Afzal, Dr. Fahad Qureshi, Dr. Shakela Bin Reyaz, Dr. Muhammad Abbas, Dr. Zakaullah Sheikh, and Assistant Prof. Jawad ul Hassan.
- My very special friend Omar Jaber Omar and his family.
- ISY support and administration departments especially Günnel Hassler and Susanna Von Sehlen.
- Some of my former teachers who always influenced and inspired me, Dr. Per Löwenborg (CTO SP Devices), Prof. Christer Svensson (IEEE Fellow), Prof. Amine Bermack (IEEE Fellow), Prof. Dr. Shoaeb A Khan, Prof. Dr. Amir Iqbal Bhatti, Dr. Nauman Mufti, Dr. Altaf Hameed, Dr. Syed Arsalan Jawed, Prof. Dr. Muhammad Javed Mirza and Squadron Leader (R) Amir Islam.
- The higher education commission (HEC) of Pakistan and Linköping university for financially supporting me.
- My loving parents for their unconditional love, prayers and moral support.
- My parents-in-law for extending their selfless help, support and love towards my family during all these four years.
- And at the end my beloved wife Dr. Saima Nawaz and my two lovely daughters Maryam and Sarah for their devotion, unconditional cooperation and extraordinary sacrifice during all these years for spending more than half of their time without me. I shall never be able to forget their extraordinary sacrifice.

Muhammad Irfan Kazim  
November 23, 2015,  
Linköping Sweden



---

## Preface

The research contributions of this dissertation carried out during September, 2011 to October, 2015 on capacitive BCC can be divided into the following three domains.

1. Investigating the capacitive BCC channel for path loss characteristics in complex scenarios and proposing a variation-aware system design simulation methodology.
2. Experimentally exploring digital baseband and passband communication for capacitive BCC channel in the context of IoT.
3. Integrated circuit design considerations for capacitive BCC AFE blocks typically low noise front end amplifiers for receivers.

Human body due to its finite conductivity and permittivity acts like a conductive channel requiring lower transmission power than air medium in the frequency range of few kHz to few MHz. The ultimate goal of the lowest power consumption for capacitive BCC transmitter/receiver can only be achieved when simple architecture consisting of only essential blocks is implemented as a monolithic single chip solution in CMOS technologies satisfying all possible communication scenarios. It is because of this reason that the two well known communication architectures, digital baseband and passband, are experimentally explored in the context of capacitive BCC channel. The physical phenomenon of signal transmission and propagation loss in complex scenarios for capacitive BCC channel is explained by the system level electromagnetic (EM) simulations. A variation-aware system design methodology based on EM simulations is proposed which defines the error bounds in terms of propagation loss variations due to natural variations in electrophysiological properties of human tissues, dielectric properties of materials/metals in close proximity and capacitive electrode coupler configurations/sizes. The effects of propagation loss due to different physical factors, as mentioned above, can be directly simulated in the circuit simulators for capacitive BCC AFE integrated circuits in the beginning of design phase to define system specifications and simplified transmitter/receiver architectures satisfying all possible communication scenarios with respect to low power.

The above mentioned research has resulted in the following published material and manuscripts.

*Paper A*

An interdisciplinary system design simulation strategy for a multidisciplinary capacitive body coupled communication (BCC) problem has been identified & formulated. A systematic, top-down, efficient, full-wave electromagnetic, variation-aware, system design simulation methodology along with 3D modeling of human body, dielectric/metallic materials, capacitive electrodes have been proposed to analyze the realistic propagation loss/path loss characteristics for capacitive BCC channel to investigate the link-budget requirements. The proposed simulation methodology has been evaluated for uncertainties due to human body dielectric properties/thickness natural variations and numeric uncertainties (boundary conditions, number of mesh cells). It has also been validated with the most reliable experimental measurement results under isolated earth conditions from the literature. The simulation methodology estimates propagation loss from 1 MHz to 60 MHz for complex scenarios due to combined interaction of the coupling electrodes, ground-plane, the material structures (metals or dielectrics) for communication distances up to 155 cm around human body.

- **Muhammad Irfan Kazim**, Muhammad Imran Kazim and J Jacob Wikner, “An efficient full-wave electromagnetic simulation for capacitive body coupled communication,” *International Journal of Antennas and Propagation*, Volume 2015 (2015), Article ID 245621, 15 pages.

*Paper B*

There are different analytical models and closed form expressions which have been derived in the literature to understand a limited or partial aspect of capacitive BCC channel. One such analytical model which was originally presented in two parts in 1936 and 1937 for determining the radiated electric field intensity on the surface of the earth due to vertical antenna configuration has been adapted to explain signal transmission mechanism as surface waves on the surface of human body. The human body is considered as an infinite half plane with dielectric properties. The proposed full-wave electromagnetic simulation methodology, which estimates the realistic path loss due to combined interaction of human body, capacitive coupler and environment, is compared with analytical closed form expression/model, to highlight the limitations as well as pros and cons of analytical modeling.

- **Muhammad Irfan Kazim**, Muhammad Imran Kazim and J Jacob Wikner, “Realistic Path Loss Estimation for Capacitive Body-Coupled Communication,” *2015 European Conference on Circuit Theory and Design (ECCTD)*, Institute of Electrical & Electronics Engineers (IEEE), 2015.

*Paper C*

The impedance of unprepared outermost skin layer varies with physical factors like age, gender, body location and humidity due to variation in thickness and

number of cells of upper epidermal stratum corneum layer of tissues. It also varies as a result of regular striping of ordinary tape and as a function of frequency. Due to high uncertainty and natural variations of outermost skin and underlying tissues impedance from person to person, it is not clearly known that how it affects the signal propagation through human body. The proposed 3D modeling and full-wave electromagnetic simulation methodology is used to determine the complex path impedance parameters due to uniform skin-only model and vertical electrode configuration as a function of different body positions from 1 MHz to 60 MHz. This helps in determining complex input/output impedance on transmitter/receiver side whose reactive component being capacitive in nature allows inductive matching for maximum power transfer. The resistive matching requirement is also greater than  $50\ \Omega$  unlike the common perception.

- **Muhammad Irfan Kazim**, Muhammad Imran Kazim and J Jacob Wikner, “Complex path-impedance estimation and matching requirements for body-coupled communication,” *2015 European Conference on Circuit Theory and Design (ECCTD)*, Institute of Electrical & Electronics Engineers (IEEE), 2015.

#### *Paper D*

In this paper, a review of current printed technologies in the context of organic thin film transistors (OTFTs) have been presented for the design of all-printed digital tag/label. On the basis of this review, a conceptual silicon-printed hybrid architecture for digital electronic tag/label in the context of IoT application has been proposed. The purpose is to simultaneously take advantage of cheaper printed OTFT technology for high cost sensors fabrication and high performance silicon based transistors for implementation of fairly complex communication paradigms. The digital tag/label is built using silicon based micro-controller to take advantage of its ultra low power modes and digital memory. Besides, printed capacitive electrodes with two distinct communication architectures; digital baseband and passband have been experimentally demonstrated/evaluated for data rates between 1 kbps to 100 kbps in isolation with earth grounded conditions for capacitive BCC channel. The simplex radio architecture has been deliberately chosen in the lab setup to isolate transmitter (which acts as a digital tag/label) from receiver which is a part of the mobile platform to gain advantage of low power consumption for digital tag/label.

- **Muhammad Irfan Kazim** and J Jacob Wikner, “Printed Electrodes with Memory Labels embracing Body-Coupled Communication – An alternate M2M Communication Paradigm for Internet-of-Things,” Submitted in IEEE Journal of Internet-of-things.

#### *Paper E*

The physical phenomenon of signal transmission for capacitive BCC channel is explained through theoretical models as well as full-wave electromagnetic

simulations for simplified human body models with uniform conductivity and permittivity. The differences with near field coupling (NFC) and Bluetooth Low Energy (BLE) technologies have also been explained in terms of reactive or radiated transmitted power. Three different communication architectures have been experimentally demonstrated and the vertical coupler configuration along with resonance tuned passband communication architecture has been found best suited for ECG measurement. This architecture is also able to transmit/receive 100 kbps data along different body positions for maximum possible communication distances on the surface of human body. It also remains unaffected by heavy clothing such as wearing jackets and binary data could even be transmitted over shoes indicating the robustness of the proposed architecture/coupling scheme against noise/interference.

- Ricardo Matias, **Muhammad Irfan Kazim**, Bernardo Cunha, J Jacob Wikner, and, Rui Martins “Capacitive Body Coupled Communication: A Step Towards Reliable Short Range Wireless Technology,” Submitted in Elsevier Microelectronics Journal.

#### *Paper F*

The low noise front end amplifier for capacitive BCC channel is built by using two-stage dominant pole split-length input transistors operational transconductance amplifier (OTA) architecture. The advantage of this OTA architecture is with respect to lower power consumption as size of compensation capacitor is reduced due to split-length transistors and compensation resistor is not required which is more sensitive to process variations. In order to address BCC channel attenuation upto 60 dB, cascading of three such OTA structures have been proposed which achieve the required transmission gain when operated as non-inverting closed loop feedback amplifiers. The OTA has been designed in a 40 nm CMOS technology for three different types of biasing techniques.

- Prakash Harikumar, **Muhammad Irfan Kazim**, and J Jacob Wikner “An Analog Receiver Front-End for Capacitive Body-Coupled Communication,” in *Proc. Norchip*, Nov., 2012.

#### *Paper G*

A low noise front end amplifier based on current-shunt, current-mirror OTA architecture is designed in a 65 nm CMOS technology for capacitive BCC receiver. The key feature of this OTA architecture is that the low power consumption has been achieved by avoiding compensation capacitors and the amplifier is used in open loop configuration without negative-feedback loop for achieving high gain in single stage. The non-linear open-loop gain is within permissible limits for digital pulse recovery for digital baseband receiver architecture. The amplifier is designed for AC coupling with the capacitive electrodes to prevent flow of conduction currents and reduce the impact of skin-electrode interface potential which appears as a DC offset voltage.

- **Muhammad Irfan Kazim**, and J Jacob Wikner “Design of a Sub-mW Front-end Amplifier for Capacitive BCC Receiver in 65 nm CMOS,” Extended abstract approved. *IBCAST*, 12–16 Jan., 2016. (Paper acceptance deadline is 25<sup>th</sup> November, 2015)

*A part of PhD research was also focused on the experimental demonstration of digital baseband and Microchip BodyCom<sup>TM</sup> scaled down version in the context of IoT application for VINNOVA, Ericsson Connected Me project, CES Las Vegas 2012, Mobile World Congress (MWC) 2012 and Motorola ATAP group now owned by Google on September 2013.*

*The following research contributions in the form of conference papers have not been included in the thesis as their contents present preliminary work which is somehow or the other included in the above mentioned publications and manuscripts.*

1. **Muhammad Irfan Kazim** and J Jacob Wikner, “Analog Signal Conditioning for Capacitive-Coupled Grounded Human-Body-Channel (HBC),” in *Proc. Swedish System On Chip Conference (SSOCC)*, Sweden, Lund, Aug., 2013. (non-peer-reviewed)
2. **Muhammad Irfan Kazim** and J Jacob Wikner, “Electrode Design Considerations for Body Coupled Communication Channel,” in *Proc. Swedish System On Chip Conference (SSOCC)*, Sweden, Linköping, Aug., 2014. (non-peer-reviewed)
3. **Muhammad Irfan Kazim** and J Jacob Wikner, “Analytical vs. Full-Wave Electromagnetic Simulation for Body Coupled Communication,” in *Proc. Swedish System On Chip Conference (SSOCC)*, Sweden, Göteborg, May, 2015. (non-peer-reviewed)

*The following research work was outside the scope of the current thesis and therefore has not been included in the thesis.*

- Jawed, Syed Arsalan and Qureshi, Junaid Ali and Ahmed, Moaaz and Shafique, Atia and Hameed, Abdul and Qureshi, Waqar Ahmed and **Kazim, Muhammad Irfan**, “A generic low-noise CMOS readout interface for  $64 \times 64$  imaging array with on-chip ADC,” *Analog Integrated Circuits and Signal Processing, Springer Science + Business Media*, 2012, 73, 273-289.



---

## Abbreviations

<b>M2M</b>	Machine-to-machine
<b>IoT</b>	Internet-of-things
<b>WSN</b>	Wireless sensor network
<b>BCC</b>	Body coupled communication
<b>RFID</b>	Radio frequency identification
<b>AFE</b>	Analog front end
<b>EM</b>	Electromagnetic
<b>NFC</b>	Near field coupling
<b>OTA</b>	Operational transconductance amplifier
<b>RF</b>	Radio frequency
<b>WBAN</b>	Wireless body area network
<b>BAN</b>	Body area network
<b>CST</b>	Computer simulation technology
<b>MWS</b>	Microwave studio
<b>RCID</b>	Resistive capacitive identification
<b>BLE</b>	Bluetooth Low Energy
<b>PCB</b>	Printed circuit board
<b>CEM</b>	Computational electromagnetics
<b>MoM</b>	Method of moments
<b>FEM</b>	Finite element method

<b>FDTD</b>	Finite difference time domain
<b>FIT</b>	Finite integration technique
<b>IBC</b>	Intra body communication
<b>EF</b>	Electric field
<b>EMC</b>	Electromagnetic compliance
<b>PBA</b>	Perfect Boundary Approximation
<b>BC</b>	Boundary condition
<b>ABC</b>	Absorbing boundary condition
<b>Str4</b>	Standard four-layer-stratified
<b>Sk-Rec</b>	Skin-only-rectangle
<b>CHI</b>	Computer human interface
<b>WAN</b>	Wide area network
<b>ECG</b>	Electrocardiography
<b>EEG</b>	Electroencyphalogram
<b>EMG</b>	Electromayography
<b>PLL</b>	Phase lock loop
<b>CMRR</b>	Common mode rejection ratio
<b>PSRR</b>	Power supply rejection ratio
<b>GBW</b>	Gain bandwidth product
<b>PHY</b>	Physical
<b>MAC</b>	Medium access
<b>HBC</b>	Human body communication
<b>PAN</b>	Personal area network

---

# Contents

<b>I</b>	<b>Background</b>	<b>1</b>
<b>1</b>	<b>Introduction</b>	<b>3</b>
1.1	Introduction . . . . .	3
1.2	Motivation . . . . .	6
1.3	Summary of Contributions to the Bulk of Research . . . . .	8
1.4	Thesis Organization . . . . .	10
<b>2</b>	<b>Capacitive BCC Challenges and Related Terminologies</b>	<b>13</b>
2.1	Introduction . . . . .	13
2.2	Capacitive BCC Challenges . . . . .	13
2.2.1	Experimental Measurement Uncertainties/Errors . . . . .	13
2.2.2	Effect of Specific Body Position and Electrode Configuration on Propagation Loss . . . . .	15
2.3	Terminologies Related with Capacitive BCC . . . . .	16
2.3.1	Quasi-Electrostatic vs Full-Wave EM Simulations . . . . .	16
2.3.2	Capacitive vs Galvanic Coupling . . . . .	17
2.3.3	Signal vs Ground Electrode . . . . .	18
2.3.4	Horizontal vs Vertical Electrode/Coupler . . . . .	18
2.3.5	Voltage vs Current Mode Driver . . . . .	19
2.3.6	Signal Termination . . . . .	20
2.3.7	Direct Coupling with Earth Ground vs Capacitive Return Path . . . . .	20
2.3.8	Effect of Ground Electrode on Capacitive Sensing . . . . .	21
2.3.9	Virtual Electrodes . . . . .	21
2.3.10	Body-to-Ground Capacitance . . . . .	22
2.3.11	Skin-Electrode Contact Impedance . . . . .	22
2.3.12	Digital Baseband vs Passband Communication . . . . .	23
2.3.13	Near Field vs Far Field . . . . .	23
2.4	Summary . . . . .	23

<b>3</b>	<b>Capacitive BCC Simulation Models</b>	<b>31</b>
3.1	Introduction . . . . .	31
3.2	Analytical Models . . . . .	32
3.2.1	Cho Analytical Model . . . . .	32
3.2.2	Ruoyu Xu Analytical Model . . . . .	33
3.2.3	Joonsung Bae Analytical Model . . . . .	34
3.3	Computational Electromagnetics (CEM) - Numerical Methods .	37
3.4	Variation-Aware System Design Simulation Methodology . . . . .	40
3.4.1	computer simulation technology (CST) Software . . . . .	41
3.4.2	Relationship of Tangent Loss as a Function of Conductivity, Dielectric Constant and Frequency . . . . .	41
3.4.3	Boundary Conditions for Stratified Human Body Model .	44
3.4.4	Variation of Dielectric with CST Fitting Models . . . . .	45
3.5	Summary . . . . .	45
<b>4</b>	<b>Electrodes, AFE Blocks and EM/Circuit Co-Simulation</b>	<b>49</b>
4.1	Introduction . . . . .	49
4.2	Application Scenarios for Capacitive BCC . . . . .	49
4.3	Electrode Design Considerations . . . . .	51
4.4	Capacitive BCC Analog Front End (AFE) Design Considerations	53
4.4.1	Design Trade-offs in the Front End Amplifiers for Receiver	55
4.4.2	Voltage Mode Driver . . . . .	58
4.5	EM/Circuit Co-simulation to Determine System Specifications .	59
4.6	Summary . . . . .	62
<b>5</b>	<b>Summary, Conclusions and Recommendations</b>	<b>65</b>
5.1	Summary and Conclusions . . . . .	65
5.2	Recommendations . . . . .	69
	<b>References</b>	<b>71</b>
	References . . . . .	71
<b>II</b>	<b>Publications</b>	<b>81</b>
<b>A</b>	<b>An Efficient Full-Wave Electromagnetic Analysis for Capacitive Body-Coupled Communication</b>	<b>83</b>
1	Introduction . . . . .	86
2	Literature Review - Modelling of Capacitive BCC Channel . . . .	87
3	Efficient Full-Wave EM Approach . . . . .	89
3.1	Coupler Configurations and Environment . . . . .	89
3.2	Human Body Modeling . . . . .	90
3.3	Simulation Setup . . . . .	90
3.4	Evaluation for Numerical/Human Body Variation Uncertainties . . . . .	91

3.5	Validation with the Measurement Results . . . . .	92
4	Simulation Results for Different Positions/User Scenarios . . . . .	94
4.1	Effect of Horizontal and Vertical Couplers . . . . .	94
4.2	Effect of Body Position, Coupler Size and Communication Distance . . . . .	95
4.3	Combined Effect of External Environment (Earth-Grounding, Material Structures) . . . . .	96
4.4	Effect of Ground-Plane on the Resultant Electric Field . . . . .	97
4.5	Link-Budget Requirement for BCC . . . . .	97
5	Conclusion . . . . .	98
	References . . . . .	108
<b>B</b>	<b>Realistic Path Loss Estimation for Capacitive Body-Coupled Communication</b>	<b>111</b>
1	Introduction . . . . .	114
2	Simplified Analytical Model . . . . .	114
3	Efficient Full-Wave Electromagnetic (EM) Model . . . . .	116
4	Comparison of Analytical and Full-Wave EM Models . . . . .	117
5	Conclusion . . . . .	118
	References . . . . .	123
<b>C</b>	<b>Complex Path Impedance Estimation and Matching Requirements for Body-Coupled Communication</b>	<b>125</b>
1	Introduction . . . . .	128
2	Proposed Efficient Full-Wave Electromagnetic Simulation Methodology . . . . .	128
3	Complex Path Impedance Estimation and Matching Requirements	132
4	Conclusion . . . . .	135
	References . . . . .	137
<b>D</b>	<b>Printed Electrodes with Memory Labels Embracing Body-Coupled Communication – An Alternate M2M Communication Paradigm for Internet of Things</b>	<b>139</b>
1	Introduction . . . . .	142
2	A Systematic Review of All-Printed Digital Memory Labels . . . . .	144
3	Architectural Descriptions . . . . .	147
3.1	Digital Baseband Communication (Architecture-I) . . . . .	148
3.2	Passband ASK Communication (Architecture-II) . . . . .	149
4	About Capacitive Electrodes . . . . .	151
4.1	Screen Printed Electrodes in the Experimental Setup . . . . .	153
5	Experimental Results . . . . .	154
5.1	Lab Setup and Instrumentation . . . . .	154
5.2	Factors Influencing Measurements . . . . .	154
5.3	Architecture-I Measurements . . . . .	156
5.4	Architecture-II Measurements . . . . .	156

6	Conclusion . . . . .	158
	References . . . . .	160
<b>E</b>	<b>Capacitive Body Coupled Communication: A Step Towards Reliable Short Range Wireless Technology</b>	<b>167</b>
1	Introduction . . . . .	170
2	About Capacitive BCC . . . . .	172
2.1	Brief Literature Review about Capacitive BCC Channel .	172
2.2	Why Capacitive Coupling? . . . . .	173
2.3	Equivalent Circuit Models for Radiation and Reactive Coupling . . . . .	175
2.4	EM Simulations for Radiated Power and Reactive Cou- pling . . . . .	176
3	Experimental Demonstration of Capacitive BCC with Three Dif- ferent Architectures . . . . .	178
3.1	Digital Baseband Architecture - LiU . . . . .	179
3.2	Microchip BodyCom Architecture . . . . .	181
3.3	Narrowband Architecture - UA . . . . .	183
4	Conclusions . . . . .	189
	References . . . . .	191
<b>F</b>	<b>An Analog Receiver Front-End for Capacitive Body-Coupled Communication</b>	<b>197</b>
1	Introduction . . . . .	200
2	Human Body Electrical Model . . . . .	200
3	Human Body Channel Characteristics . . . . .	201
4	BCC Transceiver Architecture . . . . .	202
5	Receiver Front End Architecture . . . . .	203
5.1	Sub-Blocks of the AFE . . . . .	203
5.2	AFE Topologies . . . . .	206
5.3	Simulation Results . . . . .	207
6	Conclusion . . . . .	207
	References . . . . .	209
<b>G</b>	<b>Design of a Sub-mW Front-End Amplifier for Capacitive BCC Receiver in 65 nm CMOS</b>	<b>211</b>
1	Introduction . . . . .	214
2	System Design Considerations for Capacitive BCC Front-End Amplifier . . . . .	216
3	Front-End Amplifier Design . . . . .	218
4	Simulation Results . . . . .	220
5	Conclusion . . . . .	220
	References . . . . .	222

Part I

Background



# Chapter 1

---

## Introduction

### 1.1 Introduction

A prediction of 26 billion connected devices till 2020 by Ericsson<sup>1</sup> and internet-of-things (IoT) at the peak of emerging technologies hype cycle 2014 by Gartner<sup>2</sup>, gives an insight about the future trends of technology and innovation. But the vision of future generations of connected devices is inevitable without realizing low power machine-to-machine (M2M) communication paradigms. Capacitive BCC is envisioned one of the enabling short range wireless technologies in the era of M2M communication that can meet the stringent low power consumption and transmission requirements posed by the future generations of connected devices like IoT. In the context of IoT, the futuristic scenario of smarter ambiance, where the objects could communicate by means of electronic tags/labels to “us” – the human beings; their personalized identities in the form of smart phones through capacitive BCC channel, is shown in Fig. 1.1. These electronic labels could essentially be the read-only digital memories with transmitters which must not dissipate too much power in the surroundings and transmitted signals should mostly be confined to the human body. The low power receivers integrated with the smart phones could provide an opportunity to trigger communication and receive data from digital tags/labels which could then be displayed in user friendly format on the mobile phones. The finite electrical conductivity and permittivity profile of outermost skin and underlying tissues in human body channel provide a natural opportunity to establish low transmitting power communication link between labels and “our” smart phones in the frequency range of few hundreds of kHz to few tens of MHz.

A quantitative and qualitative investigation of capacitive BCC channel for physical phenomenon of signal propagation loss, complex path-impedance

---

<sup>1</sup>Ericsson mobility report on the pulse of the networked society (June, 2015)

<sup>2</sup>The Economist, Gartner

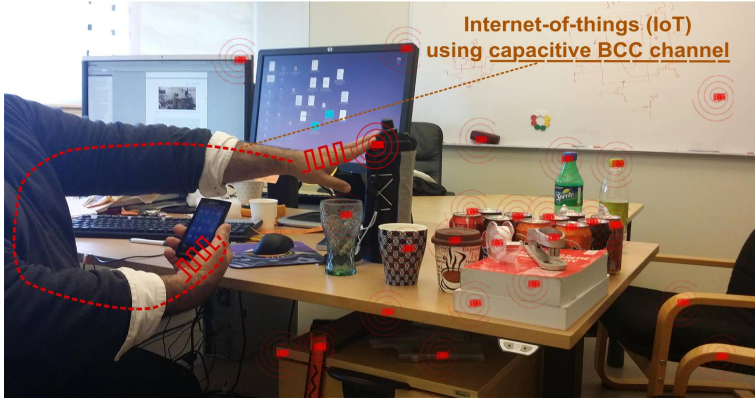


Figure 1.1: Our perceived concept of connected devices in the context of internet-of-things (IoT) using capacitive body coupled communication (BCC) channel.

estimation, system specification for suitable AFE and application scenario in the context of IoT as shown in Fig. 1.1 defines the scope of research in this thesis. A lot of research has been carried out on capacitive BCC channel to suggest suitable frequency range of operation, channel capacity for maximum data rate and power transmission requirements which are briefly discussed below from the literature survey.

T.G. Zimmerman of IBM media labs is considered pioneer for demonstrating capacitive BCC channel 20 years back in 1995 for 330 kHz carrier frequency, 30 V coupling voltage and 2.4 kbps data for foot sized personal area network (PAN) transceivers [1], [2]. Fukumoto [3] demonstrated transmission of less than 100 bps for maximum distance of 20 cm between finger ring and wrist at 91 kHz carrier frequency. He measured 3.7 dB of signal attenuation with hand touching body and 4.2 dB with hand touching ground. Handa [4] demonstrated chest to wrist channel from 10 kHz to 70 kHz with maximum transmission gain of -73 dB at 50 kHz. Hachisuka [5, 6] in contrast to Handa tested capacitive BCC signal transmission characteristics from 1 MHz to 40 MHz using earth grounded lab instruments and measured maximum transmission gain of -26 dB at 10 MHz frequency for the forearm region. He also compared human body propagation characteristics with air medium which shows that human body has almost 15 to 20 dB less attenuation for frequencies up to 30 MHz after which air medium has better transmission characteristics. Fujii [7–10] measured received voltage at a distance of 17 cm on muscle equivalent human arm phantom with electrophysiological properties valid in 10 MHz region for transmitting frequency of 10 MHz and coupling voltage of 3 V. Their results show that the maximum voltage is received when ground electrode is used at the transmitter. Yanagida [11] of Sony corporation claimed better transmission gain and low harmonic distortion for audio signal modulation in the frequency range of 500 kHz to 3 MHz. He considers that quasi-electrostatic assumption is valid

under 3 MHz and is dominant over radiation field in this range. Ruiz [12, 13] determined suitable frequency range between 200 MHz to 600 MHz for capacitive BCC channel using earth grounded signal generator and wireless communication analyzer for 20 cm and 155 cm distances. Cho [14] determined optimum frequency range between 10 MHz to 100 MHz after measuring electric field intensity from 100 kHz to 150 MHz range using battery operated transmitter but earth grounded digital oscilloscope and spectrum analyzer as receiver for 10 cm, 40 cm and 120 cm distances around both arms. According to their measurements, human body behaves as a single-pole high pass filter with cut-off frequency at 4 MHz and above 10 MHz the behavior of human body changes with frequency and distance. Schenk [15] of Philips research group presented comprehensive experimental measurement results for capacitive BCC channel as a function of different electrode configurations, human subjects and test conditions using battery operated transmitter/receiver and portable measuring instruments. Their experimental results show that the worst case body attenuation could be 80 dB for given configuration/scenario in the frequency region of 100 kHz to 60 MHz.

The brief literature survey presented above reveals the differences among the measurement results regarding the optimum frequency range, channel attenuation characteristics and data rate for capacitive BCC channel which is also influenced by electrode configuration, distance between transmitter/receiver and body positions. Despite the technical challenges posed by capacitive BCC channel, the existing short range wireless technologies based on radio frequency (RF) e.g., radio frequency identification (RFID), BLE, Zigbee, etc., are not able to meet the lower frequency range, lower power transmission/consumption requirements for low data rate applications using capacitive BCC channel [16], [17]. These RF technologies have also the risk of radiating energy, farther away than desired making it impossible to reuse frequencies and the requirement of complex protocols to setup the communication link also increases their power consumption. So, in this thesis we have mainly focused on analyzing the capacitive BCC channel both experimentally and analytically through simulations for optimum frequency and channel attenuation characteristics as a function of electrode configuration/sizes, body positions, distance between transmitter/receiver and their combined interaction with the environment. Capacitive BCC channel has also been investigated as an alternate wireless communication scheme which could meet the low power transmission/consumption and low data rate demands for special class of IoT devices such as digital memory labels/tags shown in Fig. 1.1. One of main reasons for investigating this mode of communication in this thesis is that the electrical bio-signal measurements like electrocardiogram (ECG), electroencephalogram (EEG), electromyography (EMG) and electrooculography (EOG) have the longest and the most successful track record of bioelectrical signals measurement by means of electrodes attached to the human skin. It is not necessary to place the electrodes directly on the human organ e.g., over heart in case of ECG measurement. The attenuated ECG signal can be detected by placing the electrodes elsewhere e.g., behind the ear as demonstrated in

[18, 19]. If the human heart could be considered as a biomedical implant which is transmitting signals then the attenuated signals can be measured outside the body at a different location by a receiver. This is essentially and undoubtedly an example of transmitting information through a capacitive link. The IEEE 802.15.6-2012 standard for (wireless) body area networks [20] also recognizes human body communication (HBC) channel and specifies it on the Physical (PHY) layer along with other wireless body area network (WBAN) technologies for body surface to body surface communication scenario with central carrier frequency of 21 MHz with signal bandwidth up to 5.25 MHz for data rates up to 1.5 Mbps with transmission range  $< 2$  m. The capacitive BCC is essentially a M2M communication scenario, but the human interaction makes the difference which gives a kind of real world browser like feeling to the users [21].

## 1.2 Motivation

The electrophysiological properties of outermost epidermal layer (stratum corneum), underlying dermis/subcutaneous layers, fat, muscle, cortical bone and bone marrow makes human body a low power communication channel for signal propagation in the frequency range of few hundreds of kHz to few tens of MHz. The additional advantage over the other short range wireless technologies could be of usage of frequencies, if signal confines within human body without much radiating energy in air for futuristic applications of large number of connected devices. But a brief survey of literature, presented in Section 1.1, reveals that a certain ambiguity lies regarding the experimental validation of capacitive BCC channel signal attenuation characteristics which are directly influenced by physical factors, e.g., optimum frequency range, electrode configuration/sizes, body positions, different transmitter/receiver locations and channel capacity for maximum data rate. The magnitude of signal attenuation or channel propagation loss characteristics determines the low power conditions of a communication channel. Therefore it becomes important to identify the uncertainties/errors associated with experiments for capacitive BCC channel. Most of the reported experimental measurement results fall in either of the following measurement uncertainties/errors which masks the actual propagation loss characteristics of capacitive BCC channel and sometimes original performance of transmitters/receivers as well:

1. The usage of earth grounded lab instruments.
2. Cut-off frequency limitations of analog front end (AFE) in MHz region.
3. Electrical isolation provided by using the balun with earth grounded lab instruments.
4. The measurements on simplified homogeneous muscle equivalent biological human phantoms.

It is also because of the above mentioned reasons that why any reliable solution could not be proposed so far for this mode of communication despite the first introduction was almost 20 years back in 1995 by Zimmerman [1, 2] of IBM media labs. Monolithic chip solutions in submicron CMOS technologies for capacitive BCC transceivers have been demonstrated for achieving low power consumption e.g., 5 mW for 2 Mbps [22], 0.19 nJ/b for received data [23], 2.6 mW & 0.37 nJ/b for received data [24] and 0.32 nJ/b for received data [25]. But the problem is that it is not clearly known that for how many body positions, for which coupler configuration/sizes, communication distances, environment, etc., the measured results have been reported which are very important physical factors in determining the signal propagation loss characteristics for this mode of communication. The experimental measurement setup difficulties to analyze the BCC channel for large amounts of transmitted packets under isolated earth ground conditions and to measure transmission errors as a function of natural variation of human skin and underlying body tissues from person to person also leave an ambiguity about the authenticity of given monolithic chip solutions for all possible scenarios in close vicinity around the human body.

The investigations for capacitive BCC channel have been made in this PhD dissertation by proposing an alternate system design simulation methodology to understand the physical phenomenon of signal propagation, the combined influence of electrode coupler configuration/sizes and environment (dielectric/metallic materials, earth grounding conditions) on the human body models as a uniform or as a stratified dielectric medium to realistically estimate the propagation loss for defining the link budget requirements and system specifications for AFE design of transmitter/receiver. The proposed simulation methodology has been evaluated for numeric as well as human body dielectric values/thickness variations and validated with the measured results in literature which used battery operated transceivers and portable instruments on actual human subjects to address the above mentioned experimental measurement uncertainties for larger sets of variable factors. This simulation methodology allows to estimate the complex path impedance due to uncertain and unprepared upper epidermal skin layer. The extracted S- or Z- parameters as a result of this simulation methodology allows co-simulation with the circuit simulators to define system specifications for capacitive BCC transceiver design under highly attenuated channel conditions ( $\approx 80$  dB [15] or even more [26]). Beside proposing simulation methodology, the performance of digital baseband and passband communication architectures using discrete electronic components for capacitive BCC channel in the frequency band of  $\approx 625$  kHz to 10.7 MHz for different body positions and screen printed/metallic electrodes for horizontal/vertical configuration have been experimentally demonstrated for IoT application. Both, the qualitative and quantitative results based on experimental demonstrations support simulation results.

So in the nutshell, both experimental and numeric simulation methodologies have been adapted in this PhD dissertation to understand the phenomenon and

influence of different factors on capacitive BCC channel. This information has also been utilized to define the system specifications for integrated circuit AFE design of capacitive BCC transmitter/receiver.

### 1.3 Summary of Contributions to the Bulk of Research

This PhD dissertation is an attempt to understand the signal propagation mechanism through low power capacitive BCC channel, which is so far ambiguous and not clearly known, in the presence of different physical factors which greatly affect the channel attenuation characteristics. For this purpose, the uncertainties and errors associated with the experimental characterization of the capacitive BCC channel presented in Section 1.2 have been identified after both the experimental observations/measurements and reliable simulation models. A systematic, efficient, full-wave electromagnetic, top-bottom system design, variation-aware, simulation methodology and 3D modeling of electrode coupler vertical/horizontal configuration with different sizes, human body and environment in terms of their conductivity, permittivity and tangent loss profile to estimate realistic path loss for capacitive BCC channel has been proposed in this thesis. The proposed systematic system design simulation methodology suggests an alternate strategy, not adapted before, to overcome the experimental difficulties which prevent reliable transmission/reception of large amounts of packets to analyze capacitive BCC communication link. Another difficulty in performing exhaustive experiments to estimate transmission errors is due to natural variations in human body dielectric properties from person to person due to age, gender, humidity content, body positions and coupler sizes/types. The full-wave electromagnetic analysis can be performed in any commercially available electromagnetic field simulator which supports full-wave time/frequency domain simulations but CST microwave studio (MWS) is used here for this purpose. The alternate simulation strategy allows us to,

- Estimate the realistic path loss/propagation loss due to combined interaction of human body, capacitive coupler and environment (dielectric/metallic materials) which is not provided by the analytical or empirical models thus exposing their limitations.
- Define error bounds for variations in propagation loss for numeric uncertainties (boundary conditions, mesh cells) and human body variation uncertainties (dielectric properties, dielectric thicknesses) for varying communication distances around or in close vicinity of the human body for both vertical and horizontal capacitive coupler configurations. The error bounds are within the acceptable limits for number of mesh cells, boundary conditions and variations in dielectric properties.
- Validate the most reliable measurement results presented by Philips research group [27], [15] and [28], which used battery operated capacitive

BCC transceivers and portable instruments on actual human subjects to address experimental measurement uncertainties for large sets of measurements considering variable factors. The simulation results also conform to experimental observations/measurements conducted with in-house BCC transmitter/receiver.

- Estimate the complex path impedance matrix parameters from transmitter to receiver due to uncertain unprepared upper epidermal dry layer of skin as a function of given coupler configuration, body positions and frequency range. The imaginary part of estimated, input/output equivalent impedance is capacitive in nature which allows inductive matching for maximum power transfer while the resistive matching demands higher output driver impedance  $> 50 \Omega$  up to  $\approx 1 \text{ k}\Omega$ .
- Extend the generalized “capacitive return path” theory proposed by Zimmerman [1, 2] by proving that the horizontal electrode configuration is more affected by underlying tissue variations of the human body than the capacitive return path, as compared to vertical electrode configuration. Moreover, the vertical electrode configuration can overcome the signal attenuation limitations offered by capacitive return path if the height of the vertical electrode configuration is sufficiently higher for given electrode size.
- Explain the physical phenomenon of signal transmission for complex scenarios due to the closed path loop formed by human body with the electrode couplers placed on dielectric/metallic materials with earth ground as a floor plane. It also suggests simplified skin-only rectangle human body model which reduces meshes five times compared to stratified model thus reducing the computation time to almost 10 times without much compromise on accuracy.
- Suggest a paradigm shift towards electromagnetic/circuit co-simulation for deriving system design specifications for integrated circuit design of capacitive BCC transceivers.

The digital baseband and passband communication architectures for capacitive BCC channel have experimentally been evaluated for arm-torso-arm region in the context of internet-of-things in the frequency band of  $\approx 625 \text{ kHz}$  to  $10.7 \text{ MHz}$  for different body positions and printed/metallic, horizontal/vertical electrodes configuration and sizes.

Moreover, both experimental and numeric simulation methodologies have helped to define system specifications for integrated circuit design of analog front end for capacitive BCC receiver and transmitter.

A part of PhD research was to practically demonstrate the results for digital baseband and Microchip BodyCom<sup>TM</sup> scaled down architecture and printed

circuit board (PCB) in the context of IoT application for VINNOVA, Ericsson Connected Me project<sup>1</sup>, CES LoS Vegas 2012<sup>2</sup>, Mobile World Congress (MWC) 2012 and Motorola ATAP group now owned by Google in 2013 at Linköping university. Commercially, capacitive BCC has been utilized in the form of wrist bands as a way to monitor visitors activity and interest within the Vitensenteret in Trondheim, Norway. These wrist bands are also used to customize the information provided to the visitors based on their profile<sup>3</sup>. Similarly, Swiss door lock company Kaba TouchGo<sup>TM</sup> is based on their custom resistive capacitive identification (RCID) technology which utilizes human body electrostatic properties to open door lock<sup>4</sup>. The door handle acts like the receiver electrode which is connected to digital code validation unit and transmitter is in the person pocket. However, the company uses Bluetooth Low Energy (BLE) technology for doors access with mobile phone<sup>5</sup>.

## 1.4 Thesis Organization

The general overview and organization of the rest of the thesis is depicted as follows.

- **Chapter 2** titled “Capacitive BCC Challenges and Related Terminologies” briefly explains the experimental measurement uncertainties associated with capacitive BCC channel and the effect of physical factors, e.g., body position and electrode configuration/sizes on propagation loss. The terminologies related with capacitive body coupled communication (BCC) channel have been explained e.g., quasi-electrostatic vs full-wave electromagnetic simulation, capacitive vs galvanic coupling, signal vs ground electrode, horizontal vs vertical electrode/coupler, voltage vs current mode driver, signal termination, capacitive return path, capacitive sensing, virtual electrodes, body-to-ground capacitance, skin-electrode contact impedance, digital baseband vs passband communication and near field vs far field.
- **Chapter 3** titled “Capacitive BCC Simulation Models” presents three different analytical models from the literature that cover one or more partial aspects of body coupled communication channel. They can therefore, not be treated as an alternate to experimental measurements due to incomplete and oversimplified view of some aspects of physical phenomenon related to capacitive BCC channel as compared to full-wave simulation

---

<sup>1</sup>[http://www.ericsson.com/thecompany/press/mediakits/connected\\_me](http://www.ericsson.com/thecompany/press/mediakits/connected_me)

<sup>2</sup>[http://www.ericsson.com/news/120112\\_hans\\_vestberg\\_keynote\\_speech\\_consumer\\_electronics\\_show\\_244159020\\_c](http://www.ericsson.com/news/120112_hans_vestberg_keynote_speech_consumer_electronics_show_244159020_c)

<sup>3</sup><http://www.vitensenteret.com/> ; A project by Alfredo Pérez Fernández (my research collaborator) of NTNU, Norway

<sup>4</sup><http://www.kaba.com/access-control/en/solutions/electronic-access-control-standalone-systems/81282/kaba-touchgo.html>

<sup>5</sup><http://www.kaba.com/en/kaba/654468-837342/kaba-launches-kaba-mobile-access-solutions-at-hitec.html>

methodology. The four methods of computational electromagnetics (CEM) namely, method of moments (MoM), finite element method (FEM), finite difference time domain (FDTD) and finite integration technique (FIT) are qualitatively compared. The general description of CST MWS, relationship of tangent loss in terms of conductivity and dielectric constant, effect of normal and tangential components of electric field on human stratified model and variation of dielectric properties with CST fitting model is described.

- **Chapter 4** titled “Electrodes, AFE Blocks and EM/Circuit Co-Simulation” briefly describes application scenarios and capacitive electrode design considerations for capacitive BCC channel. Low power design trade-offs are discussed for integrated circuit of front end low noise amplifier in deep submicron CMOS technologies, as it is the most important AFE block. It forms a compulsory part for both digital baseband and passband receiver communication architectures. The design of voltage mode tri state output driver on transmitter side is discussed. EM/Circuit co-simulation is performed to determine some system specification parameters for capacitive BCC channel.
- **Chapter 5** titled “Summary, Conclusions and Recommendations” summarizes and presents general conclusions from the PhD research work. It also proposes recommendations for future research.

These chapters are aimed to provide necessary background material to understand capacitive BCC in a general context and more specifically to fully understand the authors research work presented in the second part of dissertation in the form of peer-reviewed, published journal paper, conference papers and manuscripts.



# Capacitive BCC Challenges and Related Terminologies

## 2.1 Introduction

The challenges in experimental characterization of capacitive BCC channel have been briefly discussed in Sections 1.1 and 1.2 of Chapter 1. Section 2.2 explains them further with the help of illustrative figure. The general terminologies related to capacitive BCC channel have extensively been used in the literature, which are described in Section 2.3 from the authors perspective.

## 2.2 Capacitive BCC Challenges

The most common uncertainty errors regarding experimental measurements of propagation loss characteristics for capacitive BCC channel have been summarized in Subsection 2.2.1. T. G. Zimmerman, who is considered a pioneer for capacitive BCC indicated the dominance of electrostatic interactions (i.e. capacitive coupling between transmitter, receiver and human body with external earth ground) in his electrical model [1, 2]. He considered human body as a perfect electric conductor. It is explained in Subsection 2.2.2 that the physical factors like specific body positions and electrode configuration/sizes also greatly influence the propagation loss characteristics for capacitive BCC channel.

### 2.2.1 Experimental Measurement Uncertainties/Errors

Most of the experimental measurement results regarding propagation loss of capacitive body coupled communication channel reported in the literature suffer from uncertainty errors which are due to the following reasons:

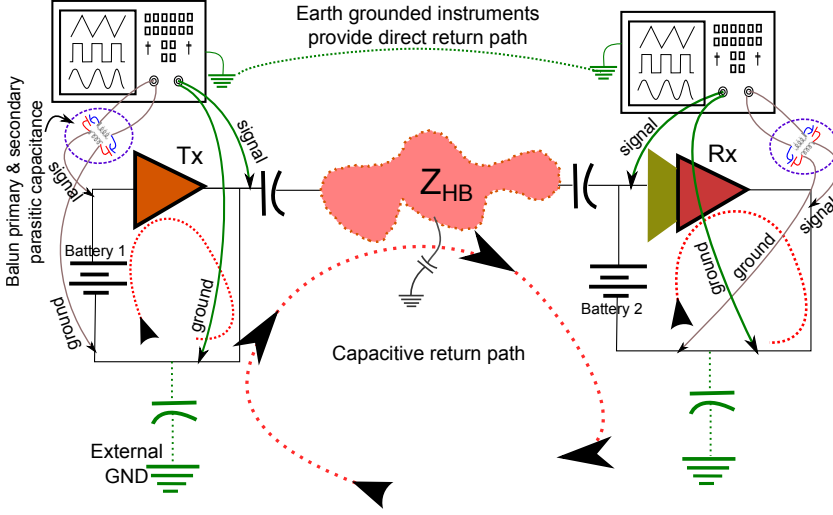


Figure 2.1: Two different scenarios related to capacitive BCC channel experimental measurement uncertainty/error, are shown in this figure. Scenario 1; when earth grounded instrument is used for measurement/probing on battery operated transmitter/receiver. Scenario 2; when the parasitic capacitance between primary/secondary coils do not provide electrical isolation for common-mode signals. Scenario 3; capacitive return path for battery operated transmitter/receiver.

- The usage of earth grounded lab instruments either on transmitter or receiver side which allows direct coupling with the earth ground as shown in Fig. 2.1.
- The first-order high pass filter response due to single RC pole formed by measuring instrument AFE (i.e. coupling capacitance and input impedance values are limiting factors) as shown in Fig. 2.2.
- The use of balun with earth grounded lab instruments to provide electrical isolation.
- The measurements performed on simplified homogeneous muscle equivalent biological human phantoms.

It is because of the above mentioned measurement uncertainties that most of the reported measurement results in the literature do not represent the real propagation loss of capacitive BCC channel. [14], [6], [29] and [30] are some of the examples from the reviewed literature whose actual human body propagation loss is masked either due to the direct return path provided by earth grounded lab instruments as shown in Fig. 2.1 or due to high pass filter cut-off frequency limitations of measuring instrument analog front end (AFE) typically in the MHz region as shown in Fig. 2.2. The battery operated transmitter or

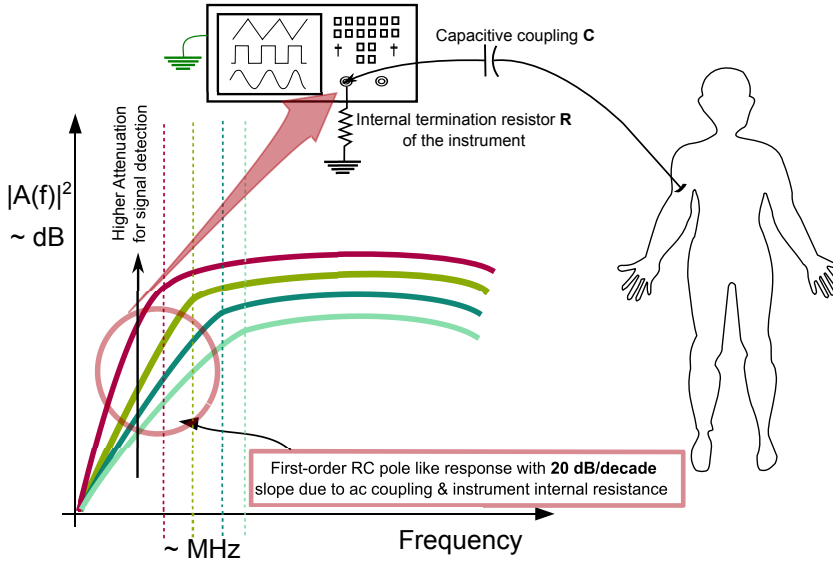


Figure 2.2: First-order RC pole 20 dB/decade like response due to analog front end limitations. The instruments internal termination resistance and coupling capacitor can mask the actual propagation loss characteristics of human body.

receiver ground is connected with instrument ground during measurements to avoid floating ground conditions. The earth grounded lab instruments used for measurements therefore improve transmission for battery operated transmitters and receivers due to their indirect coupling with earth ground as shown in Fig. 2.1. The only solution is to use battery operated instruments for measurements. The use of balun with earth grounded instruments do not provide complete electrical isolation due to the presence of parasitic capacitance between primary and secondary coils of balun which allow the coupling of common mode signal as explained in [31]. It has also been experimentally shown in [31] that the maximum difference in the magnitude of transmission gain for four different types of balun used with earth grounded instruments could be as high as 40 dB due to different values of parasitic coupling capacitance. Some of the examples from the literature which fall under this category of measurement uncertainty or experimental error are [32] and [33]. The examples of experimental measurement uncertainty for human equivalent phantoms from literature are [10] (muscle equivalent phantom at 10 MHz) and [34] (muscle simulating liquid). The homogeneous biological human phantoms mostly correspond to muscle tissue values which are accurate at one typical frequency, neglecting the effect of upper epidermal and underlying skin layers which are much more difficult to model. The unprepared upper epidermal skin layer is difficult to model due to the following uncertain characteristics.

- [35] reported that nine times stripping of stratum corneum corneocyte cell layers from cellulose adhesive tape, changes skin impedance from 200 k $\Omega$  to 1 k $\Omega$  at 1 Hz.
- [36] showed that the number of corneocyte cells, in stratum corneum upper epidermal skin layer, vary widely with body locations from individual to individual as compared to age and gender factors.
- [37] measured skin impedance variation from 10 k $\Omega$  to 1 M $\Omega$  at 1 Hz, while it was measured between 100  $\Omega$  to 1 k $\Omega$  at 1 MHz.

### 2.2.2 Effect of Specific Body Position and Electrode Configuration on Propagation Loss

The receiver sensitivity, i.e., the ability of a receiver to detect minimum input signal, is important for determining the maximum detectable range for signal transmission. That is why efforts have been made to make low noise receivers for capacitive BCC channel, e.g., [22–25]. But it is not clearly known that for how many body positions and for which coupler configuration/sizes, communication distances, environmental conditions, etc., the results have been reported, which are important limiting factors in determining the overall propagation loss. The transmission gain of BCC channel improves when earth grounded lab instruments are connected with battery operated transmitters or receivers as they provide an alternate indirect return path other than the capacitive return path as shown in Fig. 2.1. It is however not known, whether the earth grounded lab instruments were connected during the actual testing of BCC transceivers designed in [22], [23], [24], [25]. The propagation loss for capacitive BCC channel not only increases with communication distance between transmitting and receiving electrodes but it is also affected by specific body positions and the coupler configurations (i.e. coplanar horizontal and overlapping vertical) as shown in Paper A of the author [26]. For example, Table II of [26] summarizes those scenarios where propagation loss due to one body/arm position is higher than the other for the same communication distance and electrode configuration.

The graph in Figure 5a of Paper A [26] for vertical coupler configuration is explained below in greater detail to emphasize the effect of physical factors like coupler dimensions, spacing/separation between the couplers, coupler construction, coupler distance from the body, arm orientations and body movements on propagation loss measurements presented in [27], [15] and [28]. The A2A3 path is the fore arm region before elbow and A2A4 path includes the elbow region as well. All colored symbols other than triangle symbol in Figure 5a show propagation loss variations for A2A3 path. The navy blue symbols show variations due to varying coupler dimensions (3 $\times$ 3, 4 $\times$ 4, 3.5 $\times$ 5.5 with 1 cm separation and 3.5 $\times$ 5.5 with 2 cm separation). The olive green symbols show variations due to varying separation distance between vertical couplers (2 cm, 1 cm, 0.5 cm and 0.2 cm for 4 $\times$ 4 cm<sup>2</sup>). The teal color shows variations due to

vertical coupler construction (fully filled with PVC foam and/or PCB material). One of the measurements is at a distance of 1 cm from the body for A2A3 path. All coloured triangular symbols show variations for A2A4 path. The crimson colored triangles represent variations due to varying electrode dimensions ( $3 \times 3$ ,  $4 \times 4$ ,  $3.5 \times 5.5$  with 2 cm separation distance and  $4 \times 4$  with 0.5 cm separation). The dark orange triangles show variations due to different arm orientations (fore-arm bended at 90 degrees in the forward direction, arms in downward position sideways away from the body). The dark magenta triangles show variations due to body postures (sitting & standing) and body movements (walking & moving arm). However, the simulation is shown for one vertical coupler configuration [ $4 \times 4 \times 1$ ] for skin-only-rectangle human body model for both A2A3 and A2A4 paths. The graph in Figure 5b shows the dependence on the orientation of horizontal couplers (longitudinal or transversal) on the transmitter and receiver sides.

The systematic measurement variations due to different parameters of electrode coupler could be considered as a part of the design problem because it has been shown in Paper A [26] that the electrode coupler design (dimensions and type) is determined and limited by the choice of the body wearable e.g., wrist watch, pendant or ring.

## 2.3 Terminologies Related with Capacitive BCC

The following terminologies have been extensively used in the literature for capacitive body coupled communication (BCC). There also exist some differences on their usage and understanding among the authors. Here in this section, these terminologies have been explained from the perspective of author.

### 2.3.1 Quasi-Electrostatic vs Full-Wave EM Simulations

Before explaining quasi-electrostatic, it is better to define quasi-static.

Quasi-static model applies under the conditions where “the system is small compared with the electromagnetic wavelength associated with the dominant time scale of the problem.” [38]

“Quasi-statics is useful for a better understanding of the transition from statics to dynamic.” [39]

Quasi-electrostatic is a special case of quasi-static model which includes only the capacitive effects. The inductive effects are not considered or neglected in quasi-electrostatic model [39]. The Maxwells equations under quasi-electrostatic conditions, neglect  $\partial B/\partial t$  in Faradays law [39]. So the differential form of Maxwells equations under quasi-electrostatic assumption can be represented as follows:

$$\nabla \cdot E = \rho / \epsilon_0 , \quad (2.1)$$

$$\nabla \cdot B = 0 , \quad (2.2)$$

$$\nabla \times E = 0 , \text{ and} \quad (2.3)$$

$$\nabla \times B = \mu_0 \left( J + \epsilon_0 \frac{\partial E}{\partial t} \right) . \quad (2.4)$$

It is possible to directly derive equivalent circuit models from quasi-electrostatic model.

There are three main full-wave numerical methods in computational electromagnetics (CEM); namely, method of moments (MoM), finite element method (FEM), and finite difference time domain (FDTD) method. Full-wave analysis applies to situations where electromagnetic field varies over time while propagating through a medium or structure. This methodology is computationally intensive as it does not assume quasi-static conditions. As a general rule of thumb, quasi-static assumptions are valid for frequencies where object or structure size is one eighth of applied signal wavelength whereas full-wave is accurate for higher frequencies [40]. The output of full-wave analysis is in the form of scattering S-parameters in time or frequency domain [40].

### 2.3.2 Capacitive vs Galvanic Coupling

A comprehensive definition of capacitive and galvanic coupling is given in Wegmüller PhD dissertation [41].

The pioneer of capacitive coupling is T.G. Zimmerman, whose electrical model comprehensively explains that it is possible to detect the electric field at the receiver node, if the electric field is induced at the transmitter node. The transmitting and receiving signal electrodes are needed to be attached to human body. The return path of the signal is completed by the second overlapping plates of the capacitive coupler, also termed as floating ground electrodes, on the transmitter and receiver nodes which interact with the external earth ground through the air. The transmitted electric field is lowered when a human body is in direct contact with the external earth ground. The return path is dependent on the environment which is one of the main limiting factors for data rate.

In contrast, galvanic coupling is linked with injecting alternating current in the human body. The differential signal is applied through two signal electrodes so the ground reference is not much needed. But the majority current flows between the transmitting electrodes and relatively smaller current flows towards the receiving electrodes which results in greater attenuation of the signal. One of the claims about galvanic coupling is that it is less dependent on the environment [41].

Some texts in the literature refer galvanic coupling as waveguide intra body communication (IBC) and capacitive coupling as electric field (EF) IBC [30, 42].

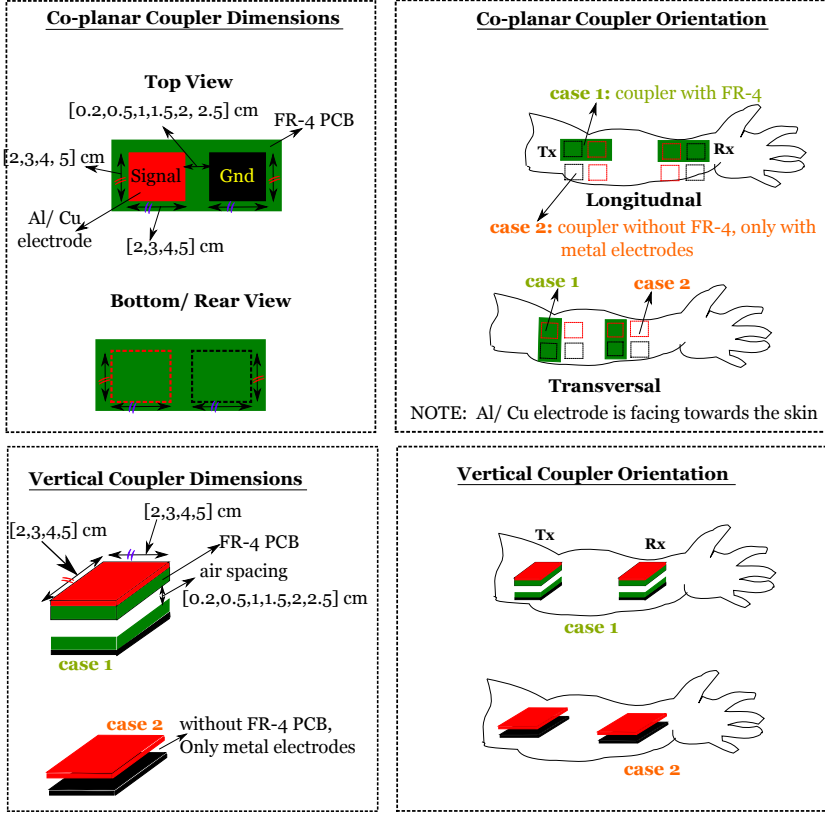


Figure 2.3: The physical dimensions and orientations of horizontal/vertical electrodes are shown. The concept of signal and ground electrodes have also been highlighted. Moreover, the horizontal electrode can be used for galvanic coupling while the vertical electrode for capacitive coupling.

The author recognizes two different electrode configurations; co-planar horizontal which is used in galvanic coupling and overlapping vertical which is used in capacitive coupling. These electrodes produce tangential and normal components of the electric field at the surface of human body when excited with electromagnetic source. Both the electric field components have different absorption inside the human body depending upon the relative permittivity of each tissue layer. This explanation is more compatible with the proposed efficient full-wave electromagnetic simulation methodology presented in Paper A [26]. The condition of applying differential current with horizontal electrode is not considered necessary in this explanation.

### 2.3.3 Signal vs Ground Electrode

The significance of ground electrode in signal transmission is evident by one of the earlier works presented in the capacitive BCC literature by Katsuyuki Fujii and Koichi Ito [7], [8], [43], [9], [10] and [44]. They explained the transmission mechanism between transmitter and receiver attached to the human arm muscle equivalent phantom of uniform conductivity and permittivity through experimental measurements. A realistic simulation model of Japanese adult male and female was also simulated using finite difference time domain (FDTD) method. It was proven that the ground and signal electrodes separated by few cm distance, placed on the surface of the muscle equivalent phantom at 10 MHz, increases the strength of the applied electrical field on the transmitter side. In this way the maximum power is coupled with the human body as compared to the situation when ground electrode is floating in air. Hwang [45] also confirmed low signal loss in the presence of the ground electrode at smaller distances. However, the signal loss decreases as the communication distance increases. The higher current density due to ground electrode was also observed. Their human arm model consisted of skin, fat, muscle, bone cortical and bone marrow tissues.

The term ground electrode was also used in the later works under the quasi-electrostatic assumptions [6], [46] and [47]. One of the inherent problems with the ground electrode is its conflicting role. On one hand, it is attached to the local ground reference of the transmitter or receiver circuit which can result in coupling of interference/noise signal from the environment to the underlying circuit, but on the other hand it provides a low impedance termination path for the capacitive fields thus avoiding the false alarms. The ground electrode, attached to the receiver, can effect the sensitivity of the receiver by loading extra body grounded capacitance at the sensitive input node of the front end amplifier.

### 2.3.4 Horizontal vs Vertical Electrode/Coupler

Capacitive coupler consists of two plates of electrodes which form an indispensable part of two structurally different capacitors and are termed as the signal and ground electrodes, respectively under quasi-electrostatic conditions. One of the electrode structures is similar in construction to the parallel plate capacitor and is formed by placing one plate of the electrode overlapping the second plate with either the dielectric medium or air in between them. The electric field is affected by the size and vertical spacing between the two plates and is referred in this thesis as vertical overlapping coupler/electrode. The other structure is formed by placing the two plates adjacent to each other in the same plane. This structure is referred by the author as co-planar horizontal electrode/coupler.

These terminologies can be related to the capacitive and galvanic coupling. The galvanic coupling can use horizontal co-planar coupler configuration for inducing electric current inside the human body whereas capacitive coupling can use vertical overlapping coupler configuration for applying electric field

Types of Capacitive Coupling schemes

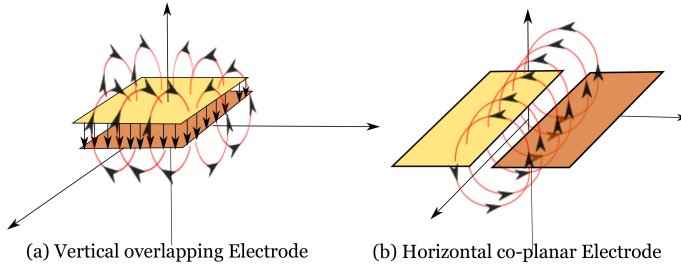


Figure 2.4: Coplanar horizontal vs overlapping vertical capacitive electrodes

potential. Capacitive or galvanic coupling also emphasizes the use of specific driver circuitry in transmitters with horizontal or vertical electrodes. The output driver in transmitter can be of two types, voltage mode or current mode as explained in 2.3.5.

### 2.3.5 Voltage vs Current Mode Driver

The voltage and current mode drivers have extensively been used in high frequency digital signaling applications which could also be motivated towards capacitive BCC. The following discussion on the voltage and current mode drivers for digital signaling is adapted from [48].

The simplest difference between voltage and current mode drivers is that the voltage mode driver has low output impedance, but the current mode driver has very high output impedance. Voltage mode drivers use Thevenin-equivalent series termination, whereas current mode drivers use Norton-equivalent parallel termination.

Voltage mode drivers switch supply voltages (power and ground) alternatively with very low output impedance to connect to the transmission line. If  $Z_0$  is the characteristic impedance of the transmission line, then on-resistance of the voltage mode driver should not be greater than approximately 10 % of  $Z_0$  for fast settling time and full-rail voltage swing. That is why MOSFET driver transistors have larger widths which also increases the gate capacitance. A predriver circuit is required to drive these large capacitive loads. Due to large gate capacitances of output transistors, delay is larger and higher power consumption in the driver and predriver stages is disadvantageous in voltage mode signaling. The implementation of voltage mode driver also depends on the requirement of output voltage swing. For example, a CMOS inverter type driver could be used in the output stage for full-rail high voltage swing. In order to avoid static power consumption, due to temporary short circuit of the supplies during high transition in the inverter type voltage mode driver, NMOS FET should be turned off before PMOS FET. This can be avoided by

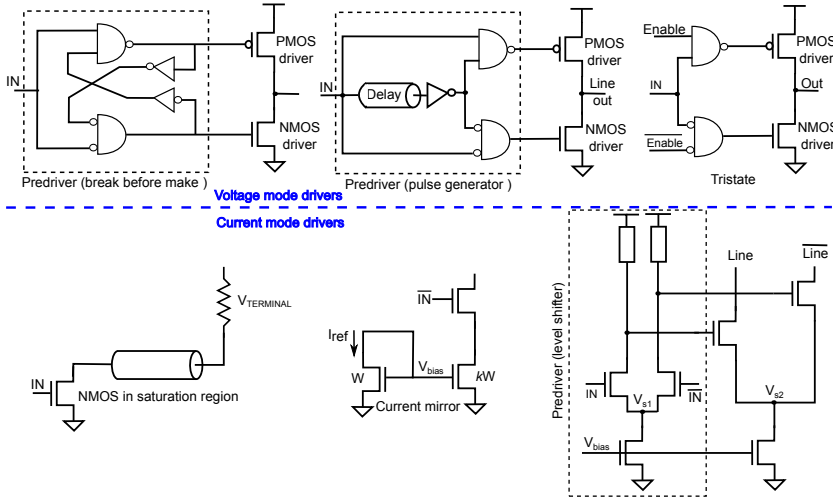


Figure 2.5: Different types of voltage mode and current mode drivers

using break before make type of predriver but it further increases the delay. Another type is, pulse generating predriver which avoids delay and reduces power consumption by pulsing-on NMOS and PMOS in the driver stage during falling and rising transitions of the input signal. When multiple voltage mode drivers share the common transmission line, then tri state predrivers are useful as they can switch to a third high impedance state when they are not driving the line. The advantage of differential mode voltage driver is that the output signal is not dependent on reference power supply and ground reference voltages as compared to the single-ended driver.

The current mode driver can be implemented by a single NMOS FET along with the transmission line and termination resistor as shown in Fig. 2.5. During on state, NMOS acts like a constant current source operating in the saturation region and output impedance is determined by the device  $(\lambda I_d)^{-1}$  characteristic. However single NMOS FET is sensitive to the process, voltage and temperature (PVT) variations. A more robust current mode driver to PVT variations can be implemented as a current mirror where the reference current is applied to the diode connected FET. Switched current drivers give a sharp transient response. Differential mode current steering driver uses limited swing, level shifted predriver which gives less than unity gain to the differential driver stage. The gain-bandwidth product of a differential stage is a constant quantity. Less than unity gain results in a very high bandwidth which causes a very fast transition. The above mentioned current mode drivers sink current from transmission line in one direction, thus forming unipolar current mode drivers.

### 2.3.6 Signal Termination

Signal reflections occur due to resistive mismatching when incident wave/signal rise/fall time becomes comparable with time of flight of a transmission line. As a result of mismatching, reflections in the form of forward and backward traveling waves occur on a transmission line. Resistive matching of transmission line characteristic impedance with source impedance ensures that backward traveling wave is absorbed on the transmitter side. Similarly, forward traveling wave gets absorbed on the receiver side, if the load impedance is resistively matched with transmission line characteristic impedance.

In case of capacitive body coupled communication, reflections are not a major issue of concern, specially in the frequency range of 1 MHz to 10 MHz.

### 2.3.7 Direct Coupling with Earth Ground vs Capacitive Return Path

According to Zimmerman electrical model [1] of the capacitive BCC channel, the body impedance can be ignored at medium frequencies. But the capacitive coupling either between transmitter local ground & external earth ground or receiver local ground & external earth ground plays an important role in successful signal transmission. Zimmerman electrical model considers the floating ground electrodes which completes the current return path through air fringing capacitance between transmitter and receiver. For smaller distances, air fringing capacitance between transmitter and receiver is effective but for larger distances, floating ground electrodes need to complete the current return path by forming coupling capacitance with the external earth ground. The current return path improves and the received signal strength increases if either the transmitter or receiver reference ground is directly coupled with the external earth ground. These concepts are elaborated in detail in Fig. 2.1 The concept of capacitive return path could be well understood by considering, “a very important aspect in the diagnosis of an electromagnetic compliance (EMC) problem, the current return path” [49]. According to this concept, all the current should return to their source through the path of least impedance. Digital signals/pulses have wide range of frequency spectrum and it is possible that some frequencies follow one path of return and the others follow another path of return. The concept of “Signal Ground” could also be better explained by this definition that instead of looking at it as zero impedance, equipotential surface it should be treated as a return path for the signal. So the signal grounds should be considered as the return path for signal currents that cover a certain loop area. In EMC problems, the larger the loop area, the higher is the radiated emission of the signal currents. Moreover, real grounds have impedance and high frequency current flows through them due to which they also result in coupling of interference. These concepts are relevant in the case of capacitive return path as well.

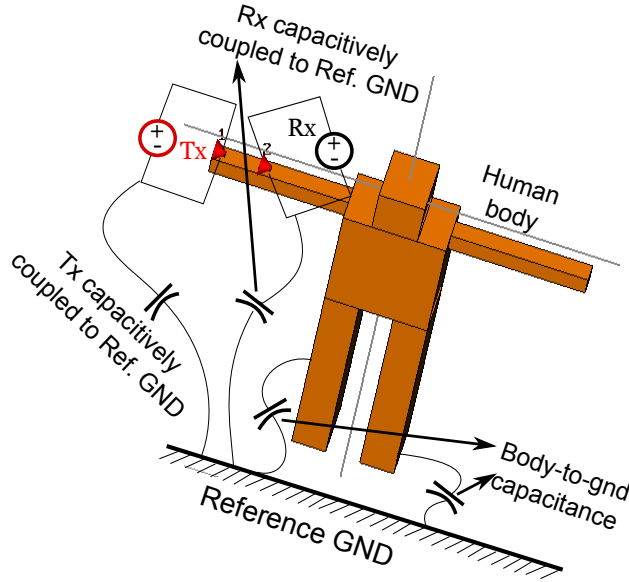


Figure 2.6: Body-to-ground capacitance refers to the coupling capacitance formed between human body and external earth ground.

### 2.3.8 Effect of Ground Electrode on Capacitive Sensing

Capacitive fields are omnidirectional and they can be detected by two conductive plates of a coplanar capacitor. One of them is connected to the electrical port which senses the change in voltage due to change in capacitance and the other one is connected to the circuit ground. The shape of sensing and ground electrodes can both be used for shaping or increasing or decreasing the sensitivity of the capacitive sense field. The grounding helps in killing the spread of capacitive fields beyond the limits of ground electrode, as it provides low impedance path for fields to terminate, thus confining them. A bigger ground plane in co-planar configuration, non-overlapping with the capacitive sense electrode, increases the overall sensitivity of the sense electrode by changing the total capacitance with respect to ground which could be explained by means of mutual capacitance formed between human body & sense electrode and human body & ground electrode. Both of these mutual capacitance vary with human body position and movement. Ground electrode is at the same time, the part of a circuit ground which acts as a reference for the entire circuit. Larger ground electrode ensures that the circuit ground is more stable and it is not influenced by the small mutual capacitance formed between human body and ground electrode. The bigger ground plane also helps in shifting the sensitivity towards the smaller capacitive sense electrode by allowing higher charge density, more concentrated flux lines and more polarization due to external object or human body.

### 2.3.9 Virtual Electrodes

Any surface which is conducting or non-conducting could act as a virtual electrode when it is either in direct contact or in close proximity with the metallic electrode. The non conducting surface in this case acts like a virtual electrode which can sense capacitive field. The lateral spreading of capacitive fields depend on the material thickness, composition, humidity content, electrode size, shape and placement of electrode on the surface, and distance from the ground surface or electrode. So the spreading of capacitive fields depend upon the conductivity/permittivity profile of the material. If the transmitter and receiver metallic electrodes are in contact with the table or some dielectric, it can enhance the capacitive fields and can also result in false alarms, if the capacitive fields are not properly terminated.

### 2.3.10 Body-to-Ground Capacitance

Under electrostatic conditions at low frequencies up to 1 MHz, stray capacitance exists between human body and external earth ground which causes conduction current to flow through the body [50]. This stray capacitance also provides an alternate path for frequencies higher than 100 kHz which is a source of error for body impedance measurements [50] in bio-medical applications. If the value of stray capacitance is larger, the current flows through this grounded capacitance without reaching the receiver. the value of body-to-ground capacitance was measured between 110 pF to 3.9 nF at different locations for different situations in [51]. In a later work, body-to-ground capacitance was experimentally measured between 136 pF to 273 pF for sitting and standing positions touching different objects [52]. The highest value for body-to-ground capacitance was found to be 3932 pF when metallic object was being touched in the standing position [52]. This shows that body-to-ground capacitance is effected when body is touching grounded objects. Common mode voltage of front end amplifier is also affected by body-to-ground capacitance and other stray impedance as measured in [52]. The value of body-to-ground capacitance has been estimated by using finite element method in [30] for capacitive body coupled communication but the maximum estimated value is 4.2 pF.

### 2.3.11 Skin-Electrode Contact Impedance

Human skin is a multilayered combination of the outermost epidermis layer, innermost subcutaneous and in between dermis layers . The epidermal layer consists of the outermost stratum corneum layer which is formed by non-conductive, dehydrated, dead cells called corneocytes. The inner layer of the epidermis has an aqueous saline environment. The non-conductive stratum corneum acts like a dielectric layer between the metallic electrode and underlying conductive tissues in an aqueous environment. Once the signal crosses the dielectric barrier, the ionic current flows in the underlying layers of skin which can be electrically rep-

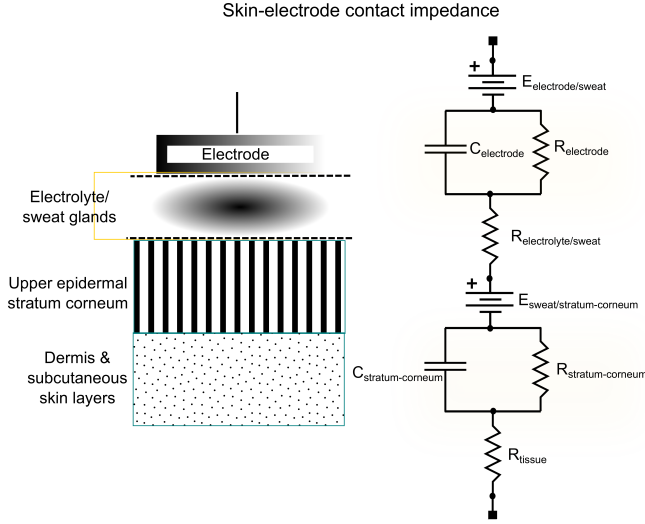


Figure 2.7: The cross-sectional view of the skin with electrode and the equivalent lumped electric circuit model for skin-electrode interface.

represented by lumped elements, i.e., parallel resistor and capacitor. Skin-electrode interface also gives rise to barrier potential. Dermis and subcutaneous tissue layers of skin can be represented by resistance. Similarly, when an electrolyte gel is used with the electrode then electrode-electrolyte interface could be represented by parallel RC lumped circuit elements. This electrode-electrolyte interface also gives rise to potential barrier. Electrolyte gel conductivity could be electrically represented by resistance. So the overall skin-electrode contact impedance for bio-medical signal measurement could be represented as shown in Fig. 2.7. Skin-electrode interface for ECG measurement has also been shown in [53] which has been adapted from [54].

### 2.3.12 Digital Baseband vs Passband Communication

The digital baseband communication refers to the transmission of digital pulse signal which is wideband in nature without carrier modulation. The driving strength of the pulse for transmission on human body can be altered using voltage mode or current mode driver as described in Section 2.3.5. If the transmitted pulses are trapezoidal in nature, then the spectral bound or spectral content is determined by the rise/fall time [55]. Therefore, it can be beneficial to implement the slew rate control in a transmitter output driver circuit. Passband communication refers to the traditional RF narrowband communication based on the sinusoidal modulation. The extreme power limitations suggest a trade off between the two modes of communication. The requirement for transmission power with digital baseband pulse communication can be very low,

as demonstrated in [22], [56], and [57].

### 2.3.13 Near Field vs Far Field

The region of near field or far field from the transmitting antenna or an electromagnetic source is normally determined in terms of radiation wavelength  $\lambda$  in free space. From this definition, if the transmitting antenna is an elementary electrical dipole then the far field starts at a distance greater than or equal to  $\frac{\lambda}{2\pi}$ . The near field is the region in free space less than  $\frac{\lambda}{2\pi}$ . The electric field due to elementary electrical dipole contains three terms  $\frac{1}{r}$ ,  $\frac{1}{r^2}$  and  $\frac{1}{r^3}$ . In the near field region,  $\frac{1}{r^3}$  term is dominant. The exponential terms of  $r^{-1}$  rapidly attenuate as the distance from the electromagnetic source increases and as a result  $\frac{1}{r}$  field dominates in the far field region.

Near field is also termed as reactive field and far field is termed as the radiative field. A comprehensive overview about these terms in the context of human body as a communication channel is given in Paper E of the thesis.

## 2.4 Summary

This chapter explains and illustrates the experimental measurement uncertainties and the effect of human body positions and electrode coupler configuration/sizes on the propagation loss variations of a capacitive BCC channel. These effects have been observed during experiments as well as during simulations. The terminologies which are essential to understand the concept of capacitive BCC channel have been discussed in Chapter 2, both from the historic and authors perspective.



# Capacitive BCC Simulation Models

## 3.1 Introduction

Chapter 2 Section 2.1 discusses the experimental measurement uncertainties associated with capacitive BCC which makes it difficult to characterize the path loss or propagation characteristics. However, an alternate approach is to model and estimate the path loss for analyzing the link budget requirements by using the circuit based models [2], [14] or the analytical/empirical models [58] or the numerical methods of CEMs [6], [46], [47], [59], [60]. The systematic, efficient, full-wave, EM, simulation methodology proposed in Paper A of the author [26] describes the effect of different physical factors like electrode configuration, body positions, human body dielectric characteristics and environment (influence of dielectric/metallic materials) on propagation loss characteristics of capacitive BCC channel especially for longer communication distances  $> 50$  cm<sup>1</sup>. A comparison of this simulation methodology with a comprehensive analytical model presented in [58] has been carried out in Paper B of the author [61]. The proposed simulation methodology has also been used to estimate the parameters  $Z_{11}$ ,  $Z_{12}$ ,  $Z_{21}$  and  $Z_{22}$  of complex path impedance matrix in Paper C of the author [62] as a function of different body positions to estimate the impedance matching requirements for maximum power transfer from transmitter to receiver.

Chapter 3 describes the analytical models available in the literature which are useful to understand the partial aspects of human body channel characteristics. But these analytical models do not provide the full insight about the realistic propagation loss characteristics due to combined interaction of capacitive electrode coupler, human body (considering the electrophysiological properties of skin and underlying tissues) and dielectrics/metals in the environment as compared to the proposed simulation model. The different numerical

---

<sup>1</sup>Majority of the literature on capacitive BCC channel reports results for  $< 50$  cm.

methods of computational electromagnetics (CEM) for solving the Maxwell equations namely, method of moments (MoM), finite element method (FEM), finite difference time domain (FDTD) and finite integration technique (FIT) are qualitatively compared in tabular form. FIT forms the basis of CST MWS numerical field solver and simulation tool which is used for the proposed EM analysis. The relationship of tangent loss,  $\epsilon'$  (real) and  $\epsilon''$  (imaginary) is defined as they describe the important dispersive properties of the materials. The parametric model to describe the dielectric properties of different human tissues also use these parameters. The EM CST MWS also use tangent loss,  $\epsilon'$  and  $\epsilon''$  for material properties. The variations in the dielectric properties with respect to CST MWS internal fitting curves are also discussed.

## 3.2 Analytical Models

The analytical models for capacitive BCC channel are based on the empirical formulas which gives relationship for one or more physical parameters. They do not give the complete design picture but gives useful insight about the physical phenomenon from design perspective.

### 3.2.1 Cho Analytical Model

It is well known from Zimmerman electrical model [1, 2] about capacitive BCC channel that the capacitive coupling of transmitter/receiver local grounds with the external earth ground plays an important role in the return path of the current. It considers human body as a perfect conductor having no impedance. The distributed RC model presented in [14], is based on the electrical equivalent model of extracellular and intracellular tissues. It considers the conduction current and voltage drop inside the human body and supports capacitive return path. Cho has also derived the relationship in [14] for determining the minimum ground plane size on PCB referred as  $A_{\min}$  for battery operated transmitter. His empirical formula relates the minimum ground plane with empirical constant  $K$ , carrier frequency  $f$ , communication distance  $D$ , receiver sensitivity  $S_{Rx}$  and transmitted power  $P_{Tx}$ . The following analytical expression has been derived in [14]:

$$A_{\min} = \frac{S_{RX}}{P_{TX}} \frac{(1 + f/f_0)^P}{(1 + f/2f_0)^2 (Kf)^2}, \quad K = 3 \times 10^{-9}; \quad (3.1)$$

$$f_0 = \frac{10 \times 10^6}{D}, \quad P = \begin{cases} 4 & D > 0.8 \\ 3. & \text{else} \end{cases} \quad (3.2)$$

As an example, the minimum ground plane requirement on PCB, for a receiver sensitivity of -70 dBm, transmitting power of -10 dBm and for a communication distance of 1 m at 10 MHz carrier frequency can be calculated as 79 cm<sup>2</sup> from

this formula. However, the experimental measurements have been carried out using earth grounded instruments on the receiver side for deriving this empirical formula. The high pass filter cut-off frequency is approximately 10 MHz due to single RC pole, which is a measurement artifact due to the front end instrument limitation. The actual propagation loss characteristic of human body channel is in fact masked due to constant slope of 20 dB/decade up to 10 MHz.

### 3.2.2 Ruoyu Xu Analytical Model

Ruoyu Xu analytical model [42] is based on a simplified voltage divider rule to determine the received voltage  $V_{RX}$  from transmitted voltage  $V_{TX}$ , transmitter output impedance  $Z_{TX}$ , receiver input impedance  $Z_{RX}$ , return path impedance  $Z_{return}$  and body impedance  $Z_{body}$ . It is given by (3.3). It neglects the leakage impedance due to the signal loss in the presence of earth ground. It is evident from (3.3) that the maximum amplitude can be received, if the receiver input impedance  $Z_{RX}$  is high. The return path impedance should also be minimized. The analytical expression is given by

$$\frac{V_{RX}}{V_{TX}} = \frac{Z_{RX}}{Z_{TX} + Z_{RX} + Z_{body} + Z_{return}} \approx \frac{Z_{RX}}{Z_{body} + Z_{return}}. \quad (3.3)$$

In order to find the return path impedance, it is important to find the expression for the coupling capacitance between transmitter/receiver ground and external earth ground. (3.4) is valid only for parallel plate capacitors when distance ( $d$ ) between the plates is much less than the surface area ( $S$ ) of the plates meaning by it neglects the effect of the fringing capacitance. It is given by

$$C_{plate} = \frac{\epsilon_r \epsilon_0 S}{d}. \quad (3.4)$$

The parallel plate capacitance, when distance ( $d$ ) between the plates become comparable to the surface area ( $S$ ) and fringing capacitance can not be ignored, is given by (3.5) in [42] whose original derivation can be found in [63]

$$C_{plate} = K \left( \frac{d}{l} \right) \frac{\epsilon_r \epsilon_0 l^2}{d}, \quad (3.5)$$

$$K(b) = \begin{cases} 1 + 2.343b^{0.891}, & 0.1 \leq b < 1.0 \\ 1 + 2.343b^{0.992}, & 1.0 \leq b < 10.0 \end{cases} \quad (3.6)$$

In (3.6),  $b$  is the ratio between distance  $d$  and length  $l$  of the parallel plate.  $K(b)$  is the empirical ratio between  $C_{plate}$  calculated from (3.5) and parallel plate capacitor calculated from (3.4). Square plates have been assumed in this derivation. If transmitter/receiver ground planes on PCB could be modeled as square plates with height  $h$  above the external earth ground, then the capacitance between the original plate and its image is twice the parallel plate capacitance

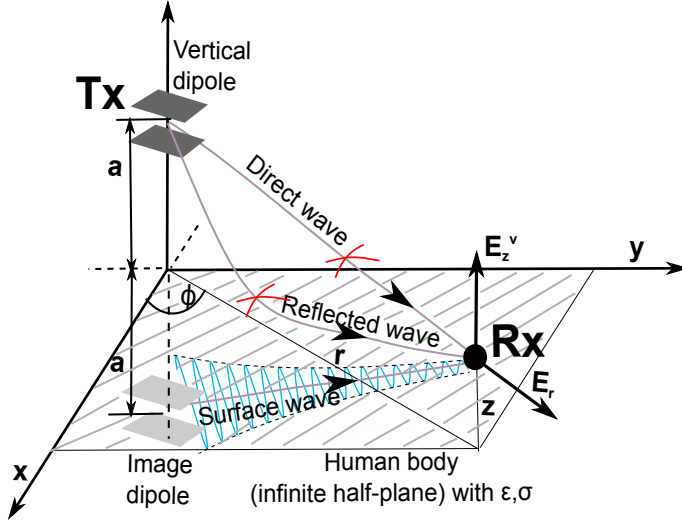


Figure 3.1: Conceptual analytical model presented in [58] for capacitive BCC where human body is modeled as infinite half plane.

with  $d$  equal to  $2h$  as shown in (3.7)

$$C_{\text{GND}} = 2 \cdot K \left( \frac{2h}{l} \right) \frac{\varepsilon_r \varepsilon_0 l^2}{2h} = K \left( \frac{2h}{l} \right) \frac{\varepsilon_r \varepsilon_0 l^2}{h}. \quad (3.7)$$

However, it has been argued that the actual value of grounded capacitance could even be less than predicted by (3.7) because of the human body shielding effect, which had not been taken into account during this derivation. The lower value of grounded capacitance in the return path results in increased body channel attenuation.

### 3.2.3 Joonsung Bae Analytical Model

The Bae analytical model presented in [58] explains the physical phenomenon of signal transmission through capacitive BCC channel. It uses the analytical expressions derived in [64] and [65] which calculate the radiated electric field intensity from a vertical antenna at the surface of the earth. Bae assumes the human body as an infinite half-plane. The electrical properties of the infinite half-plane depend on frequency, conductivity and permittivity profile of skin and underlying tissues in human body whose dielectric values have been used from [66]. The transmitter electrode is assumed as an infinitesimal dipole which has an image dipole due to infinite half-plane assumption. The conceptual analytical model is shown in Fig. 3.1. The difference from the actual model presented in [64], [65] is, it has been assumed for capacitive BCC that the space wave is zero due to vertical dipole. Therefore direct and reflected waves, which are

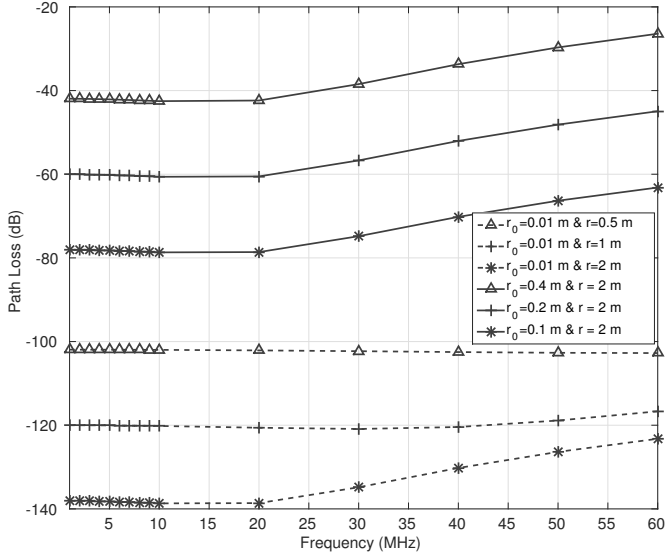


Figure 3.2: Path loss vs frequency (MHz) plot for Joonsung Bae analytical model [58] for different dipole lengths and communication distances.

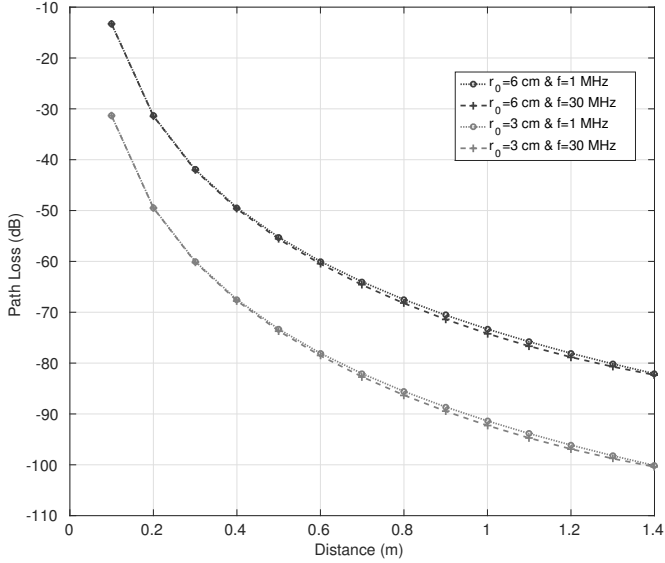


Figure 3.3: Path loss vs distance (m) plot for Joonsung Bae analytical model [58] between two different dipole lengths at 1 and 30 MHz.

the subcomponents of the space wave, cancel out each other due to the vertical dipole placed on the surface of a human body. The surface wave predominates as shown in Fig. 3.1. The surface wave travels along the curvature or surface of the body because of the process of diffraction [64]. Surface wave induces voltage on the body surface which results in surface wave attenuation as it moves away from the transmitting electrode. The attenuation of the surface wave expressed as  $(1 - u^2 + u^4)F$  in (3.8) depends on the communication distance  $r$ , frequency (wave number  $k = 2\pi/\lambda$ ) and dielectric properties (conductivity  $\sigma$  and complex permittivity  $\epsilon$  values) of the underlying tissues in a human body. The vertically polarized surface waves are less in contact with the body surface as compared to the horizontally polarized surface waves, which travel parallel to the body surface. So the vertically polarized surface waves suffer lesser attenuation and variations due to lesser dependence on tissue dielectric properties, as also proven by efficient full-wave simulation methodology [26]. The following analytical expressions (3.8) are used from [58] to plot the path loss from 1 MHz to 60 MHz in Fig. 3.2 and 3.3, respectively. It is assumed  $a = z = 0$  and  $\sin \psi' = z + a/R_2 = 0$ ,

$$\frac{|E_z v(r, k)|}{|E_z v(r_0, k)|} = \left| \frac{k(1 - u^2 + u^4)F(r, k) \cdot \frac{1}{r} + j \cdot \frac{1}{r^2} - \frac{1}{k} \cdot \frac{1}{r^3}}{k(1 - u^2 + u^4)F(r_0, k) \cdot \frac{1}{r_0} + j \cdot \frac{1}{r_0^2} - \frac{1}{k} \cdot \frac{1}{r_0^3}} \right|, \quad (3.8)$$

where,

$$\begin{aligned} F &= 1 - u^2 e^{p_2 - p_1} - u \theta e^{-p_1} \int_{\sqrt{p_2}}^{\sqrt{p_1}} \frac{e^{\omega^2}}{\sqrt{\omega^2 + \theta}} d\omega, \\ u &= (\epsilon + jx)^{-1/2}; x = 1.8 \cdot (10^{10} \sigma / f)(\sigma / \omega \epsilon_0), \\ p_1 &= ikr[1 - (1 + u^2)^{-1/2}], \\ p_2 &= ikr[u^{-1} - (1 + u^2)^{-1/2}], \\ \theta &= 2ikr(1 + u^2)^{-1/2}; R_v = -1, \text{ and} \\ \omega &= 4p_1 / (1 - R_v)^2. \end{aligned}$$

There are certain limitations of this analytical model which undermines the results under certain scenarios. The surface wave attenuation factor  $F$  is almost constant from 1 MHz to 60 MHz as calculated in Table I of [58]. It shows that the surface wave propagation is almost independent of the human body conductivity and permittivity values, which is not true [59]. In order to obtain the closed form of  $F$ , the analytical expression in (3.8) is true under certain approximations. These are; the reference distance of vertical dipole  $r_0$  should be much less than the wavelength  $\lambda$  and communication distance  $r$  should be greater than the wavelength  $\lambda$  as calculated in Table 3.1. Similarly the analytical expression considers infinitesimal dipole and neglects the actual electrode dimensions. The limitations on  $r$  and  $r_0$  have been calculated in Table 3.1 in the frequency region of interest for capacitive BCC. The path loss of more than 100 dB is estimated due to infinitesimal dipole which has been taken almost 100 times smaller than  $r$ , plotted from (3.8) in Fig. 3.2. The path loss have also been plotted for much bigger dimensions of vertical dipole almost 10 times smaller than  $r$ . Fig. 3.3 shows the plot for infinitesimal dipole at 1 MHz and 30 MHz respectively as  $r$  is varied. The exponential curve for shorter channel distance shows that the

Table 3.1: The limitations on  $r$  and  $r_0$  of analytical model in the frequency range of 1 MHz to 60 MHz.

Frequency (MHz)	$\epsilon_r$ (Dry Skin)	$\lambda^* = \frac{c}{f\sqrt{\epsilon_r}}$	$r^* > \lambda$	$r_0^* < \lambda$ (100 times)
1	990.76	9.529	$r > 9.50$	0.095
5	579.21	2.493	$r > 2.50$	0.025
10	361.66	1.577	$r > 1.60$	0.016
20	209.22	1.037	$r > 1.05$	0.010
30	152.94	0.808	$r > 0.81$	0.0081
40	124.35	0.673	$r > 0.67$	0.0067
50	107.17	0.579	$r > 0.58$	0.0058
60	95.736	0.511	$r > 0.51$	0.0050

\* The units for  $\lambda$ ,  $r_0$  and  $r$  are in meters.

path loss is inversely proportional to the third order of distance and for larger distances ( $> 0.8$  m), it is linearly proportional on the channel distance.

### 3.3 Computational Electromagnetics (CEM) - Numerical Methods

computational electromagnetics (CEM) provides a numerical solution for problems involving electromagnetic (EM) interaction (i.e. E (Electric) and H (Magnetic) fields computation) over complex physical structures whose analytical or empirical solution is not possible. CEM can be broadly categorized into numerical methods and high-frequency methods; the former is used for the scenarios where the physical size of an object is comparable to the wavelength whereas the latter is used in situations where the physical size is much bigger than the wavelength. The numerical methods can be classified on the basis of differential or integral equation which can be subdivided into frequency or time domain [67].

The electromagnetic simulators employ one or more numerical methods and the main purpose is to find an approximate solution to Maxwell equations that satisfy a given set of boundary conditions and initial conditions. The simulation process starts with the creation of physical model (geometrical/material parameters) and EM simulation set-up (boundary conditions/ports). The EM simulation is performed afterwards which discretizes the physical model using ‘mesh cells’. The unknown field/current is approximated using an expansion or basis function whose coefficients are adjusted until the boundary conditions are satisfied.

Considering the range of applications and problem areas, there is no one

solution or method which fits all the application areas perfectly. In principle, different methods can be used to solve the same problems, however, there are often good reasons why one particular simulator is better suited to solving a particular problem type. The commonly used numerical methods are, method of moments (MoM) (based on integral equation and frequency domain), finite element method (FEM) (based on differential equation and frequency domain), finite difference time domain (FDTD) (based on differential equation and time domain) and finite integration technique (FIT) (based on integral equation and time-domain) [67]. Although the discussion about these numerical methods lies outside the scope of this thesis, the comparison among the popular solvers (MoM, FEM, FDTD and FIT) are tabulated in Table 3.2.

Table 3.2: Summary & comparison of MoM, FEM, FDTD and FIT (TD).

Figure-of-merit	MoM	FEM	FDTD	FIT (TD)
<b>Classification</b>	FD, integral eq.	FD, differential eq.	TD, differential eq.	TD, integral eq.
<b>Solution Method</b>	implicit	implicit	explicit	explicit sol. of Maxwell eq.
<b>Discretization</b>	Surface (only metals)	Volume (full-domain)	Volume (full-domain)	Volume (full-domain)
<b>Core Unknowns</b>	Current distribution (metal surface)	electric/magnetic field (whole solution space)	electric & magnetic fields (whole solution space)	electric & magnetic fields (whole solution space)
<b>boundary conditions (BCs)</b>	No special BC	absorbing boundary condition (ABC)	ABC	ABC
<b>Broadband frequency</b>	single or few	single or few	Well-suited	Well-suited
<b>N-port structure</b>	Well-suited	Well-suited	Not Well-suited	Not Well-suited
<b>Typical Applications</b>	'3D' planar structures metallic antennas	3D arbitrary multi-chip modules	3D arbitrary bio/EM	3D arbitrary antenna on human/aircraft

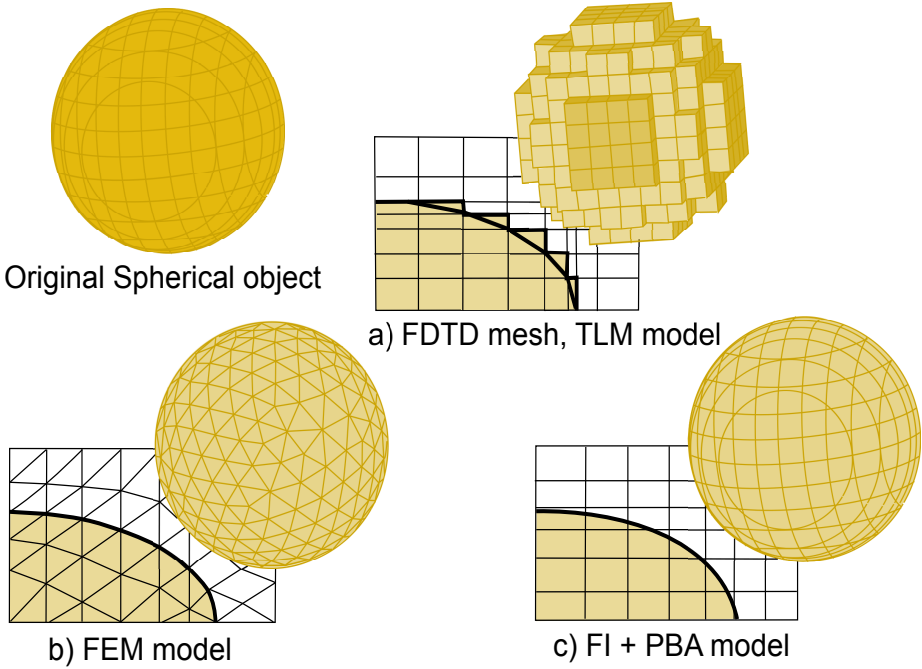


Figure 3.4: EM modeling of curved surfaces exposing the limitations of numerical methods as shown in [68].

### 3.4 Variation-Aware System Design Simulation Methodology

Variation-aware efficient full-wave electromagnetic (EM) simulation methodology is described in detail in Paper A of the author [26] with the extension of work in papers B [61] and C [62]. The concept of a full-wave electromagnetic simulation is based on electrical polarization of human body due to propagation of EM waves to explain the phenomenon of signal loss inside the human body. It can mathematically be expressed by the relationship of tangent loss and attenuation constant as a function of effective conductivity, permittivity and frequency which can be found in any standard textbook of electromagnetics [69]. The importance of this relationship is also in the context of modeling human body either as a stratified or skin-only medium which also gives advantage in terms of computation cost without compromising the accuracy. The full-wave EM field analysis has been carried out in 3D EM tool of computer simulation technology (CST) microwave studio (MWS) which is based on the finite integration technique of computation electromagnetics.

### 3.4.1 CST Software

CST MWS is a general purpose electromagnetic solver which is based on FIT [68]. This numerical method can be applied to a wide range of frequencies from DC to high frequency. CST is able to perform accurate modeling of curved structures by utilizing perfect Boundary Approximation (PBA) as illustrated in Fig. 3.4. The combination of FIT algorithm with PBA allows much better approximation of complex geometries as compared to FEM which allows segmentation or FDTD which performs stair case approximation as illustrated in Fig. 3.4. The transient solver of CST MWS allows to perform simulation over wide frequency range in a single computation time. These simulations are suited for open boundary conditions as well as large dimensions. Moreover, the mesh influences the accuracy as well as the speed of the simulation and it can be done manually and automatically. In the context of capacitive BCC, which involves the complex interaction of coupling electrodes, the environment and the human body from 1 MHz to 60 MHz, a broadband response is required which can be achieved using a transient simulation. The FIT with PBA technique of CST MWS seems to be a natural choice.

### 3.4.2 Relationship of Tangent Loss as a Function of Conductivity, Dielectric Constant and Frequency

Biological tissues and cells are lossy in nature and this lossy nature determines the propagation behavior of the EM waves passing through them. The fundamental question is that how loss which is expressed as tangent loss, is interrelated with conductivity and dielectric constant in biological tissues. A lossy biological tissue  $\sigma \neq 0$  means that when EM wave passes through it, there is a power loss of the propagating wave which will produce heat. In order to better understand the loss of propagating wave through biological tissue, we state the time harmonic version of the Maxwell equation which is

$$\nabla \times \overline{H} = \overline{J}_c + j\omega\epsilon\overline{E} , \quad (3.9)$$

where  $\overline{J}_c = \sigma_c\overline{E}$  is the conduction current caused by the application of an external electric field and  $\sigma_c$  is the conductivity which describes the mobility of free electrons. Under the influence of an external electric field  $\overline{E}$ , the electrical dipoles inside the biological material align themselves with the field and results into electric flux density. (3.9) can therefore be rewritten as

$$\nabla \times \overline{H} = \sigma_c\overline{E} + j\omega\epsilon_0\epsilon_r\overline{E} , \quad (3.10)$$

where  $\epsilon_r$  is the relative permittivity of the biological tissues which is a complex quantity. Relative permittivity characterizes the interaction of dipoles in a biological tissue with the applied electric field. The dipole repeatedly aligns itself with the alternating applied electric field according to the correct polarity and as a result of rotational motion of dipole and rapid acceleration and deceleration,

energy is lost in the form of heat. The out of phase property of the dipole with the incident electric field is determined by the real part of permittivity expressed as  $\epsilon'$ . The oscillatory motion of dipoles which results in signal energy loss in the form of heat is determined by the imaginary part of the relative permittivity expressed as  $\epsilon''$ . Therefore we can replace  $\epsilon_0\epsilon_r = \epsilon' - \epsilon''$  in (3.10) which gives us

$$\nabla \times \bar{H} = \sigma_c \bar{E} + j\omega(\epsilon' - \epsilon'')\bar{E}, \quad (3.11)$$

$$\nabla \times \bar{H} = (\sigma_c + \omega\epsilon'')\bar{E} + j\omega\epsilon'\bar{E}, \quad (3.12)$$

$$\nabla \times \bar{H} = \sigma_e \bar{E} + j\omega\epsilon'\bar{E}, \quad (3.13)$$

where  $\sigma_e = \sigma_c + \omega\epsilon''$  is the effective conductivity with  $\sigma_c$  as the static conductivity and  $\omega\epsilon''$  is the conductivity due to applied time harmonic field. Returning back to Maxwells (3.13),

$$\nabla \times \bar{H} = j\omega\epsilon'(1 - j\frac{\sigma_e}{\omega\epsilon'})\bar{E}, \quad (3.14)$$

$$\nabla \times \bar{H} = j\omega\epsilon'(1 - j\frac{\sigma_c}{\omega\epsilon'} - j\frac{\epsilon''}{\omega\epsilon'})\bar{E}, \quad (3.15)$$

$$\nabla \times \bar{H} = j\omega\epsilon'(1 - j\tan\delta_e)\bar{E}. \quad (3.16)$$

$\tan\delta_e$  in (3.16) is defined as the loss tangent which has two contributing terms. The first term  $\frac{\sigma_c}{\omega\epsilon'}$  describes the loss due to collision of electrons with other atoms. For example *Copper*,  $\sigma_c = 5.8 \times 10^7 S/m$  implies that charges flow easily without collision. Large conductivity implies almost zero electric field intensity as in case of copper. The second term  $\frac{\epsilon''}{\omega\epsilon'}$  of the loss tangent depicts that how much energy supplied by an external electric field is dissipated as heat due to oscillatory motion of dipoles under the influence of alternating field. This term usually dominates in dielectrics. Most of the bio-materials do not fall in either high or low loss tangent materials. They have in fact moderate loss tangents where both conduction (due to  $\sigma_c$ ) and displacement (due to  $\epsilon_r$ ) currents play important role. The above derivation can be found in any standard text book of electromagnetics such as [69], [70].

The above derivation of tangent loss and its relationship in terms of  $\epsilon'$  and  $\epsilon''$  is important in the context of CST MWS as the software accepts the normalized values of  $\epsilon'$  and  $\epsilon''$  with respect to  $\epsilon_0$  in the dispersion list of material properties. The dielectric values of major human body layers such as skin, fat, muscle, cortical bone and bone marrow as shown in Fig. 3.6 are based on the dielectric parametric model expressed by Debye equation and four Cole-Cole type dispersion parameters presented in [66] and [71]. The values from this parametric model are compared with the full range of experimental and literature data presented in [72] and [73] and is accurate within 1% discrepancy above 1 MHz.

The attenuation constant  $\alpha$  expressed as nepers per meter is a measure of the exponential decrease in magnitude of the EM wave as it propagates through

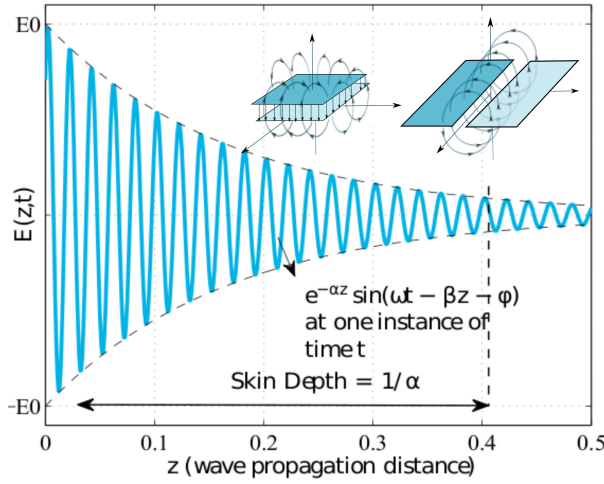


Figure 3.5: Planar wave of the form  $E(z, t) = E_0 e^{-\alpha z} \sin(\omega t - \beta z - \phi)$ . As the wave passes through a lossy material like human body, the peak magnitude decreases exponentially given by  $e^{-\alpha z}$  which is the envelope and skin depth is given by  $1/\alpha$  [70].

a biological material as shown in Fig. 3.5. It could be expressed in terms of permittivity and conductivity of the biological material, human body in our case and the propagating frequency [70]

$$\alpha = 1/\delta = \omega \sqrt{\frac{\mu\epsilon}{2} \sqrt{1 + \frac{\sigma_e^2}{\omega\epsilon'}} - 1} \cdot (Np/m) \quad (3.17)$$

Another related term is the propagation constant which determines that how much EM wave suffers from the phase shift which is expressed in radians as it passes through the biological material. It also depends on permittivity and conductivity of the biological material and the propagating frequency [70]

$$\beta = \omega \sqrt{\frac{\mu\epsilon}{2} \sqrt{1 + \frac{\sigma_e^2}{\omega\epsilon'}}} \cdot (rad/m) \quad (3.18)$$

### 3.4.3 Boundary Conditions for Stratified Human Body Model

Human body can be divided into five major layers starting from the outer most layer of skin, fat, muscle, cortical bone and finally bone marrow as shown in Fig. 3.6. Each layer has its own dielectric properties and conductivity which are also frequency dependent. In order to satisfy the Maxwell equations, the boundary conditions between different layers must be satisfied. When  $E$  field

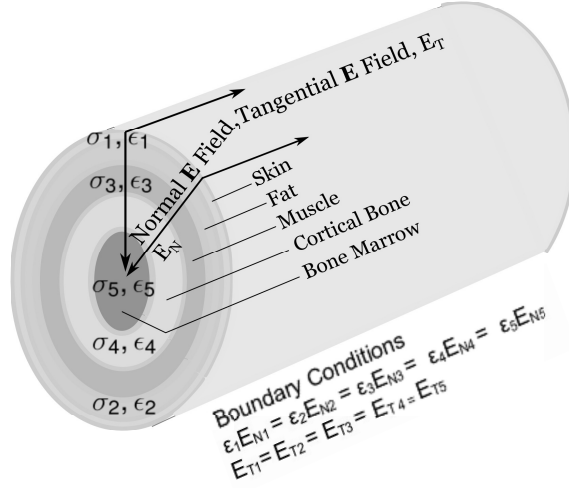


Figure 3.6: Cross-sectional view of human-arm divided into five layers: skin, fat, muscle, cortical bone & bone marrow; each having its specific  $\sigma_e$  &  $\epsilon_r$ . E field required to be satisfied by the Maxwell equations at the interface of two boundaries with different  $\sigma_e$  &  $\epsilon_r$

is applied on the exterior layer of the skin, it can be resolved into two components. The parallel component is called the tangential electric field  $E_T$  and the perpendicular component is called the normal electric field  $E_N$ .

In order to satisfy the Maxwell equations, the boundary condition for the tangential component of the electric field requires to satisfy the following equation [70]

$$E_{T1} = E_{T2} = E_{T3} = E_{T4} = E_{T5} . \quad (3.19)$$

(3.19) indicates that if we neglect the reflections and attenuation by the lossy tissues then as a first-order approximation, we can assume that the tangential field passes through the layers unperturbed at low frequencies. According to the Maxwell equation, the normal component of the electric field requires to satisfy the following boundary condition [70]

$$\epsilon_1 E_{N1} = \epsilon_2 E_{N2} = \epsilon_3 E_{N3} = \epsilon_4 E_{N4} = \epsilon_5 E_{N5} . \quad (3.20)$$

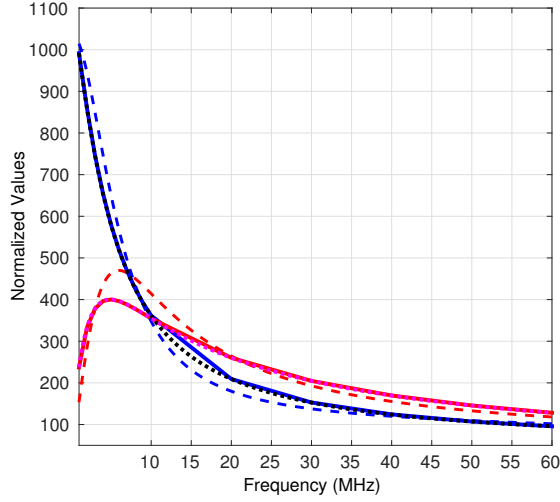
Where  $E_{N1}$  is the normal component of E field in  $\epsilon_1$  medium,  $E_{N2}$  is the normal component of E field in  $\epsilon_2$  medium and so on. (3.20) indicates that the normal component of the  $E$  field is changed by the ratio of the relative permittivity formed by the boundary of two adjacent layers and this condition is required to be true only at the boundary between the two layers. For example, the  $E$  field may change significantly within the individual layers of skin, fat, muscle and bone.

### 3.4.4 Variation of Dielectric with CST Fitting Models

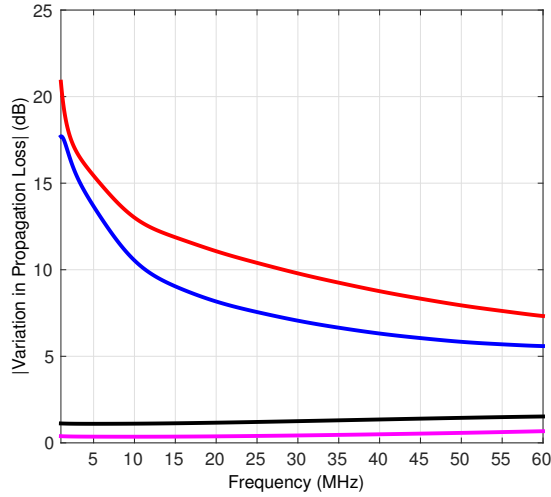
The effect of variation of dielectric dispersive properties with respect to data-fitting models of CST software is investigated. The normalized complex permittivity that is, normalized  $\epsilon'$  (real) and normalized  $\epsilon''$  (imaginary) values are compared for 2<sup>nd</sup> and 8<sup>th</sup> order fitting models with the user-defined values in Fig. 3.7a (only dry-skin is shown). Figure 3.7b shows the relative difference in propagation loss variation between standard four-layer-stratified (Str4) and skin-only-rectangle (Sk-Rec) for vertical and horizontal coupler configurations. It can be observed from the transient solver simulation results that the relative difference in propagation loss variations between Str4 and Sk-Rec is within 1 dB for vertical coupler configuration over 20 cm distance from 1 MHz to 60 MHz. However for the horizontal coupler configuration, the difference is comparatively larger as shown in Fig. 3.7b.

## 3.5 Summary

An overview is given about some analytical models presented in the literature which gives partial information about different physical factors influencing the signal propagation mechanism through capacitive BCC channel. Unlike, the proposed efficient full-wave EM simulation model characterizes the capacitive BCC channel due to combined interaction of different physical factors giving a more realistic information about the channel propagation loss. Since the proposed EM simulation model uses tangent loss,  $\epsilon'$  and  $\epsilon''$  for material dispersive properties, so their relationship is derived and explained in detail. Lastly, the variation of dielectric with different CST fitting models is considered for vertical/horizontal electrode coupler configurations.



(a)



(b)

Figure 3.7: Normalized complex permittivity that is, normalized  $\epsilon'$  (real) and normalized  $\epsilon''$  (imaginary) values of dry-skin for different data-fitting models; user-defined values [ $\epsilon'$  (solid blue),  $\epsilon''$  (solid red)], 2<sup>nd</sup> order fitting-model [ $\epsilon'$  (dashed blue),  $\epsilon''$  (dashed red)] and 8<sup>th</sup> order fitting-model [ $\epsilon'$  (dotted black),  $\epsilon''$  (dotted magenta)], (b) Variation in propagation loss among skin-only-rectangle (Sk-Rec) and standard four-layer-stratified (Str4) human arm models for distance of 40 cm with vertical couplers [6 x 6 x 3] and horizontal couplers [5 x 2 x 1]; vertical couplers [2<sup>nd</sup> order (magenta), 8<sup>th</sup> order (black)], horizontal couplers [2<sup>nd</sup> order (red), 8<sup>th</sup> order (blue)].





# Electrodes, AFE Blocks and EM/Circuit Co-Simulation

## 4.1 Introduction

Capacitive BCC is an alternate short range wireless technology which can be used under almost all those proximity scenarios where RFID or NFC applications can be envisioned. Therefore, in the first part of Chapter 4, an overview of some of those applications is given which can be envisioned using this mode of communication with a typical focus on IoT applications. The essential physical layer building blocks for digital baseband and passband communication architectures have been discussed. The system specific requirements of voltage/current mode drivers on transmitter side and front end amplifier on the receiver side have been discussed. The effect of different values of output resistance for voltage mode driver and input resistance/capacitance for receiver amplifier is shown through circuit/electromagnetic simulations which is an important step towards the realization of practical transceiver design for capacitive body coupled communication (BCC).

## 4.2 Application Scenarios for Capacitive BCC

Capacitive BCC can be envisioned as an alternative technology to the conventional optical bar codes. The advantages can be, avoidance of direct line of sight communication, both read/write capability on capacitive BCC tags/labels and high density data storage in the form of digital memories. Capacitive BCC tag/label can effectively be conceived around a single silicon based micro-controller architecture as shown in Paper D of the thesis which allows different low power modes of operation e.g., sleep, stand by, without clock, etc., to save

the power when data transmission is not done. However, the power consumption increases during the transmission mode. With the advent of ultra low power consumption micro-controllers introduced by Ambiq Micro<sup>1</sup> that operate in the nano-amperes current region due to near subthreshold operation of all digital transistors, is a practical step towards the realization of thin film battery based tags/labels. Low power capacitive BCC channel can further reduce the power as compared to RFID and NFC technologies by offering a simpler receiver architecture based on the simplex mode of communication containing less number of analog precision building blocks as compared to RFID/NFC. Capacitive BCC is shown to be more power efficient than NFC from the transmission perspective with the help of EM simulations in Paper E of the thesis. Digital labels/tags based on capacitive BCC technology can be used in the supermarkets for consumer products to increase the customer satisfaction. If all the product information written on the wrapper of the products is also digitally stored on the associated digital tags then customers can take advantage of faster electronic search for specific inquiries using their smart phones. For example, a customer looking for lactose free products can perhaps take better advantage of the digital search once the product information is downloaded on the personal smart phone. Similarly, the products from all-vegetarian source could better be inquired from the digital search of ingredients which may otherwise be a harder job to figure out from the limited products information. Similarly, the provision of a translated version of the product information in international languages in the application layer of smart phone can greatly enhance the shopping experience for the international customers. The simplex communication architecture for capacitive BCC channel can also be used either in the context of IoT or tracking of perishable items for measuring physical parameters like the minimum/maximum temperature, humidity, etc., with sensors during the logistics supply chain. Capacitive BCC due to its relatively simple communication architecture can also be implemented in the printed technologies which are still evolving today as discussed in Paper D of the thesis. However, the cost advantage of fabricating cheap sensors in printed technologies and high performance of silicon transistors for the implementation of capacitive BCC communication architecture on silicon based micro-controller can give a good compromise between cost and performance as discussed in Paper D of the thesis. The other interesting applications could be in the context of computer human interface (CHI) scenario where users can experience real world browser by physically touching a certain object and transferring a hyperlink about that typical object through capacitive BCC to the user smart phone device which uses wifi or other wide area network (WAN) technology to open the hyperlink in a browser. Similarly, unique digital code for opening door locks can be transferred using capacitive BCC channel. A commercial example of this application is in the form of Swiss door lock company Kaba TouchGo<sup>TM</sup> custom RCID technology as mentioned in Section 1.3 of Chapter 1.

---

<sup>1</sup><http://ambiqmicro.com/low-power-microcontroller>

## 4.3 Electrode Design Considerations

Historically, biomedical electrodes have been used for the purposes of bioelectrical signals detection like electrocardiography (ECG), electroencephalogram (EEG), electromyography (EMG), etc., impulses stimulation like electric nerve stimulation and recent electrical impedance tomography for human body AC impedance measurements. Similarly, the design of electrodes greatly influences the detection of signals on the receiver side, when an external current/voltage signal is applied on the transmitter side for capacitive BCC channel. One of the problems is that electrodes are normally considered as the last part in the overall electronic system design but unfortunately they influence the overall system performance in a number of ways. When the electrode comes in contact with the skin, it gives rise to a skin-electrode contact impedance and skin-electrode barrier potential. If the potential mismatch between two branches of differential electrode is larger than a few hundred mV, then differential amplifier can saturate. However, if the mismatch is smaller, then it gets amplified with the bio signal causing a level shift in the output. If contact impedance is large as compared to the input impedance of differential amplifier then signal attenuation occurs due to the voltage divider effect. The contact impedance shows frequency dependence. At low frequency, the value of the contact impedance is high which results in a greater signal attenuation which reduces as the frequency increases. This frequency dependent behavior is like a high pass filter due to the presence of a parallel plate capacitor in the electrical modeling of electrode-electrolyte or electrode-skin interface (in the absence of electrolyte). Power line interference at 50/60 Hz present in air gets capacitively coupled with the human body which produces displacement currents and cause a voltage drop across the skin-electrode contact impedance. These are some of the problems for the electrodes which are attached to the receiver. On the transmitter side, however, the electrode constraints are different as they are required to couple maximum electric field around or inside the human body by injecting current or voltage. The impedance matching requirements on the source or transmitter side become important for the maximum power transfer. It is, therefore, important to find out the impedance of the electrode. The impedance of the electrode is not only affected by its layout design but an uncertainty factor is also added due to impedance loading when it is placed on the surface of human body or skin. The electrical properties of the electrodes are therefore of great importance for capacitive BCC application. One of the important design considerations is the choice of electrode material, e.g., Ag-AgCl has not only good electrical properties specially when used with electrolyte gel (low electrode potential, low skin-electrode impedance) but also bio-compatibility.

When a metal electrode comes in contact with an electrolyte, the exchange of electrons and ions takes place as a result of the electrochemical reaction. Metal atoms lose electrons as a result of oxidation and become positively charged, whereas some positive metal ions gain electrons to deposit metal on the electrode. As a result, certain potential difference exists between electrode and electrolyte interface which is termed as half-cell. A double layer of positive and negative

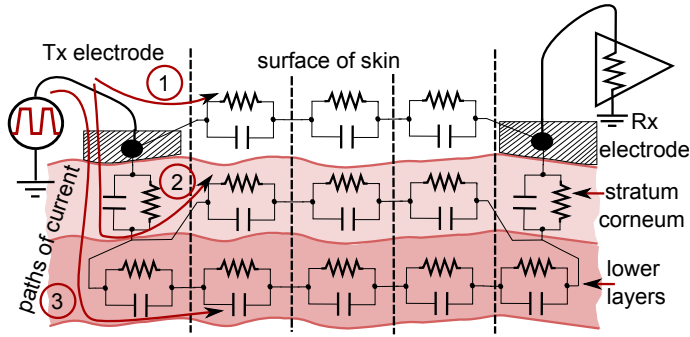


Figure 4.1: Skin-electrode contact impedance

charges is formed across the electrode-electrolyte interface which acts like a parallel plate capacitor. Due to the electrochemical reaction, the leakage of faradaic currents occur across the interface which can be modeled by a parallel resistor. No electrochemical reaction takes place when the stimulus current flows through the capacitor. The electrolyte and lead resistances can be modeled in series with a parallel RC circuit due to the electrode-electrolyte interface. Skin-electrode interface could also be modeled as a parallel plate capacitor due to the upper epidermal thick layer of stratum corneum which acts like a dielectric medium between conducting metal electrode and underlying conducting tissues of the epidermis layer of skin which have relatively aqueous environment. Hair follicles and sweat ducts present on the upper epidermal layer of skin provide parallel paths for the flow of extracellular current which can be modeled as a high resistance in parallel to capacitor. The detailed cross-sectional view of the electrode-electrolyte interface with surface potentials is shown in Fig. 2.7 but three different paths of current from transmitting electrode to the receiving electrode are shown in Fig. 4.1. It is difficult to determine from Fig. 4.1 that the current will flow along which transmission path or how much percentage of current will flow from each of the three paths to reach receiver unless the whole path impedance is not known which has been attempted to estimate in Paper C of the thesis. The mean electrode potential for six different types of screen printed electrodes under electro-chemical conditions in physiological saline solution is measured between 53 to 59 mV as shown in Fig. 4 of [74]. The median absolute maximum value of the electrode impedance is 1 k $\Omega$  at 50 Hz and it reduces to approximately 200 to 250  $\Omega$  for silver and 570 to 580  $\Omega$  for carbon conduction line electrodes as shown in Fig. 5 of [74]. However, the difference is that the screen printed electrode is used as a dry capacitive electrode in case of capacitive BCC application. So, the impact on electrode potential is expected to be lesser as compared to the electrode usage in the presence of an electrolyte or as an electrochemical half-cell in physiological saline.

Similarly, shielded cables or twisted wires are used with the electrodes to avoid magnetically induced interference [75], [76]. It has been shown in [77]

that the shielded design of screen printed EEG electrodes by a grounding layer, dramatically improves the immunity to radiated **EMI!** (**EMI!**) and powerline interference.

## 4.4 Capacitive BCC Analog Front End (AFE) Design Considerations

There are two basic communication architectures which have been experimentally demonstrated using discrete electronic components in the context of printed electrodes and capacitive BCC channel as described in Paper D of the thesis which are not necessarily the best architectures. One of the architectures is based on digital baseband communication, inspired by the Ethernet (10BaseT) half duplex standard for 10 Mbps throughput. It uses the Manchester data encoding scheme which allows simple clock recovery without using phase lock loop (PLL) and transmission of separate clock signal. This architecture does not require an analog-to-digital conversion. The absence of non-linear components, e.g., mixer, further lowers the power consumption. Because of all digital transmission, the linearity of analog components in the signal conditioning path is least important. The other architecture is based on passband communication which uses Microchip BodyCom<sup>TM</sup> commercial solution. The main receiver board has been modified to make a scaled down version for mobile platform which can send packets through Bluetooth interface. The important differences between digital baseband designed in-house and Microchip BodyCom<sup>TM</sup> passband communication architectures is that the latter has taken advantage of higher transmission voltage due to the LC resonant driver circuit, carrier modulation of digital baseband signal, highly selective bandpass filtering on transmitter and receiver sides, low sensitivity receiver and retransmission of transmitted data to enable communication through BCC channel. The digital baseband architecture lacks all these components. It transmits a digital bit stream without filtering and after amplification of high pass filtered pulses, it regenerates pulses by a digital comparator and using an oversampling architecture it recovers the transmitted clock and data. The purpose of demonstrating both the architectures is to reduce the number of essential analog building blocks from a low power consumption point of view.

Since the front end low noise amplifier is an indispensable part of a majority receiver architectures for capacitive BCC channel, therefore its most important performance parameters along with certain design trade-offs have been discussed in Section 4.4.1.

### 4.4.1 Design Trade-offs in the Front End Amplifiers for Receiver

The low noise front end amplifier constitutes one of the most important building blocks in most of the capacitive BCC communication architectures which have been demonstrated so far in CMOS technologies, e.g., [22], [56], [57], [23], [24],

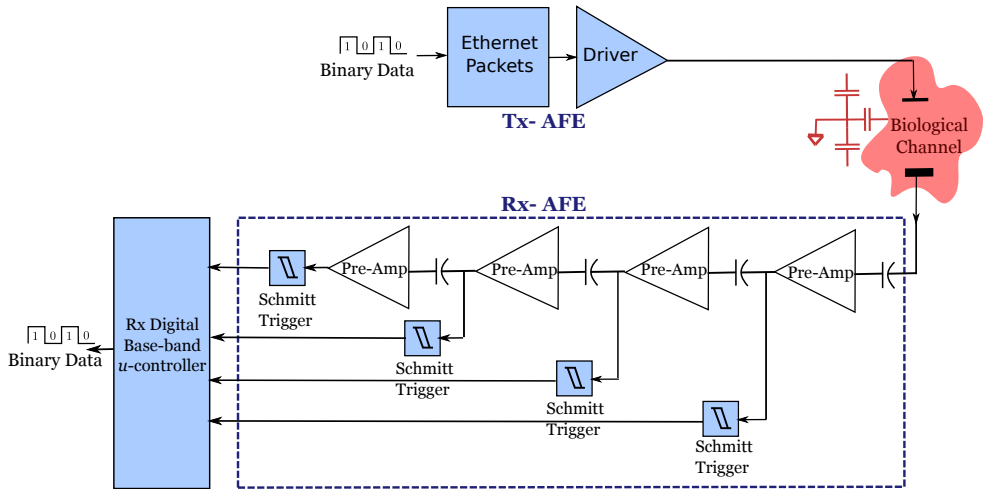


Figure 4.2: Block diagram of digital baseband communication AFE.

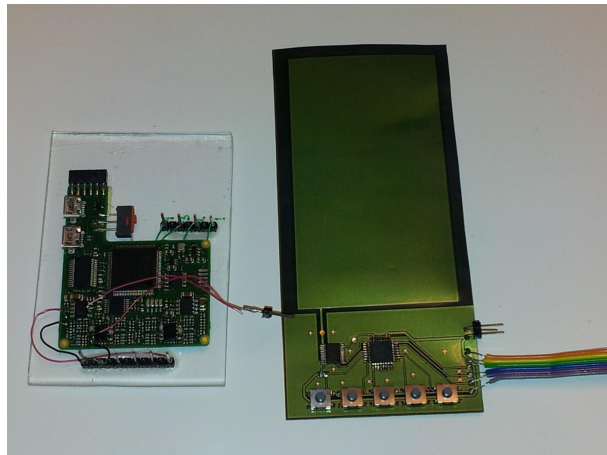


Figure 4.3: Left: digital baseband communication receiver AFE and Xilinx FPGA on PCB; Right: transmitter with micro-controller, driver and electrode.

[78], [79], [25], [80], [81] and [82]. It is important to define the right specifications at the system level when designing low noise front end amplifier for capacitive BCC channel because its design influences the entire receiver chain. The cut-off frequency for determining the -3 dB bandwidth and 0.1 dB flat gain response are two essential front end amplifier specifications but before this, a suitable frequency range for signal propagation is needed to be properly defined and understood for capacitive BCC channel. In fact there are different views in the literature about the suitable frequency range, some of which have already been discussed in Section 1.1. A frequency range of 1 MHz to 60 MHz has been used for simulating the propagation loss characteristics of the capacitive BCC channel in [26] because the dielectric properties, i.e., conductivity, permittivity and tangent loss of skin and underlying tissue layers are available with an accuracy of 1 % above 1 MHz but below 1 MHz the accuracy between measurements and parametric model is approximately 25 % less [66]. IEEE 802.15.6-2012 standard [20] recognizes human body communication channel and defines the center frequency of 21 MHz for transmission. [27] defines quite broader range of frequencies from 100 kHz to 100 MHz as suitable for signal transmission through human body. But the human body starts radiating or receiving signals like an antenna as the frequency increases above 40 MHz [78] which makes the transmission/reception at higher frequencies difficult. Hachisuka [5] measures air as a better medium of transmission than human body as a communication channel at frequencies above 30 MHz. Yanagida [11] recommends frequencies between 500 kHz to 3 MHz for audio signal transmission at 48 kbps in a patent filed by Sony Corporation. The frequency of RFID standard is defined at 13.56 MHz. The in-house experiments have been performed in the lab with 625 kHz, 1.25 MHz, 3 MHz, 5 MHz, 10 MHz, 10.7 MHz frequencies using discrete components for baseband and passband communication. If the hardware implementation is not a limiting factor, then the frequencies from 500 kHz to 10 MHz are suitable for capacitive BCC channel depending upon the data rate and the power consumption requirements.

After defining a suitable frequency range, the requirement for the front end amplifier of 0.1 dB bandwidth turns out to be 10 MHz and -3 dB bandwidth around 12 MHz to 15 MHz. The design experience in Papers F [83] and G [84] of the thesis suggest that the single pole roll-off frequency with 20 dB/decade demands a much higher unity gain frequency and directly influences the noise bandwidth. Even for a modest dc gain of 40 dB and a -3 dB bandwidth of 12 MHz, two decades of frequencies are required on a logarithmic scale with 20 dB/decade roll-off to reach unity gain frequency of 1.2 GHz which in turn increases the noise bandwidth many times. It is also mentioned in [85] that the integrated noise in a given bandwidth is an important parameter for wide band systems.

Since the capacitive BCC receiver is needed to be integrated with mobile platform, therefore low power consumption is a necessary requirement. Another criteria of low power consumption for capacitive BCC comes from the health

conditions, e.g., it is defined in *IEEE standard for safety levels of human exposure to radio frequency RF electromagnetic fields* [86] that the maximum possible electric field exposure for whole body is  $1842/(\text{frequency in MHz})$  V/m from 1 MHz to 30 MHz which could cause adverse health effects. According to ICNIRP guidelines [87], the reference current level for time varying contact currents from a conductive object is 20 mA above which shock and burn hazard could take place.

Besides low power consumption, [27] and [15] have experimentally measured a high degree of channel attenuation for the human body when the transmitter and receiver are both ambulatory devices operated with batteries and this attenuation factor could be as high as 80 dB. In fact it has been shown with EM simulations in [26] that attenuation factor can be even higher depending upon the size and configuration of the coupling electrodes, distance and location of transmitter/receiver from each other and the environmental factors. Sodini [88] has experimentally shown that the channel transmission gain measured with the grounded instruments and battery operated instruments, respectively are entirely different from each other. The difference between the two measured transmission gains is approximately 80 dB at 10 MHz which gradually reduces to 35 dB at 150 MHz. So the receiver amplifier needs to provide high gain for battery operated devices.

There is also a similarity between capacitive BCC receiver and amplifiers used for biomedical applications such as vital signs measurement. Front end amplifier in capacitive BCC receiver requires a low input referred noise for signal detection from transmitter just like the front end amplifier for biomedical measurements as described in [89]. But the additional challenge is of achieving low input referred noise at higher frequencies in MHz region with a higher bandwidth which is more difficult to design.

Common mode rejection ratio (CMRR) and power supply rejection ratio (PSRR) are other important parameters for the front end amplifier design as indicated by [90]. It has been shown in [51] and [91] that even for battery operated front end amplifiers used for biomedical measurements, the power line frequencies at 50/60 Hz and their second and third harmonics get capacitively coupled with the human body which set up conduction currents inside the human body giving rise to both differential and common mode interference signals. [51] has also calculated the values of these stray capacitance between human body and earth ground/power supply which vary with body positions and ungrounded/grounded environmental conditions.

Capacitive BCC front end amplifier is attached at the input of the capacitive electrode which is placed on the surface of the human body. The effect of electrode-skin offset potential and impedance becomes important to consider as discussed in [92] and [90] which should not be ignored. It is, however, understood that the impact of electrode offset potential is higher for electrodes which use electrolyte gel due to the electrochemical reaction [93] as compared to the capacitive electrodes. The values of screen printed electrode potentials have

been discussed in Section 4.3. AC coupling is helpful in preventing the voltage drop due to electrode impedance by blocking the conduction currents due to electrostatic coupling of power supply mains with the human body and other dc currents flowing through the body [94].

The importance of low supply voltage in a digital system for low power consumption pioneered in [95] and [96] is evident from (4.1) [97] which shows the dependence of power consumption on output node switching activity  $\alpha$  in a single clock cycle in a digital circuit, clock frequency  $f_c$  and square of supply voltage  $V_{dd}$ <sup>2</sup>

$$P = \frac{1}{2} \alpha f_c C V_{dd}^2 . \quad (4.1)$$

However, voltage scaling in analog amplifier design does not help much in reducing the power consumption [96]. Instead, the low power consumption of transistor in amplification mode depends upon the noise bandwidth  $B_n$ , output load capacitance expressed in terms of minimum capacitance implementable in a given technology  $C_{min}$ , the output voltage swing  $V_{FS}$  and the voltage gain  $A_v$  as given by (4.2) derived in [97]:

$$P = 4B_n C_{min} V_{eff} V_{FS} A_v . \quad (4.2)$$

The conventional front end amplifier design for capacitive BCC uses a 2-stage OTA in a negative feedback loop to form a non-inverting amplifier by taking advantage of the linear gain as in [83], [56]. The Miller compensated fully differential 2-stage OTA is not load compensated but uses an internal compensation capacitor for closed loop stability between the two stages which results in higher power consumption. In this case, the drawn current determines the power consumption instead of supply voltage scaling which depends on given gain bandwidth product (GBW), load capacitor  $C_L$  and overdrive voltage ( $V_{GS} - V_{TH}$ ), given by (1) and derived in [98]:

$$I_{MillerOTA} = GBW \cdot \pi \cdot (V_{GS} - V_{TH}) \cdot (8C_M + 6C_L) . \quad (4.3)$$

Common mode interference is also caused by two different ground references. A higher CMRR of the entire system is helpful in rejecting the interference in the form of common mode noise voltage due to different grounds. CMRR of the amplifiers is maximum at DC but falls at higher frequencies due to stray capacitance. The total common mode rejection ratio  $CMRR_T$  does not only depend upon the amplifier CMRR  $CMRR_{AMP}$ , but also on the ratio of common mode input impedance  $Z_c$ , electrode impedance  $Z_e$  and their relative differences  $\Delta Z_e$ ,  $\Delta Z_c$  as given by (4.4) derived in [94] and [99]:

$$\frac{1}{CMRR_T} = \frac{1}{CMRR_{AMP}} + \frac{Z_e}{Z_c} \left[ \frac{\Delta Z_e}{Z_e} + \frac{\Delta Z_c}{Z_c} \right] . \quad (4.4)$$

#### 4.4.2 Voltage Mode Driver

A general overview about voltage and current mode drivers is given in Section 2.3.5. Their importance in the design is evident from the discussion about

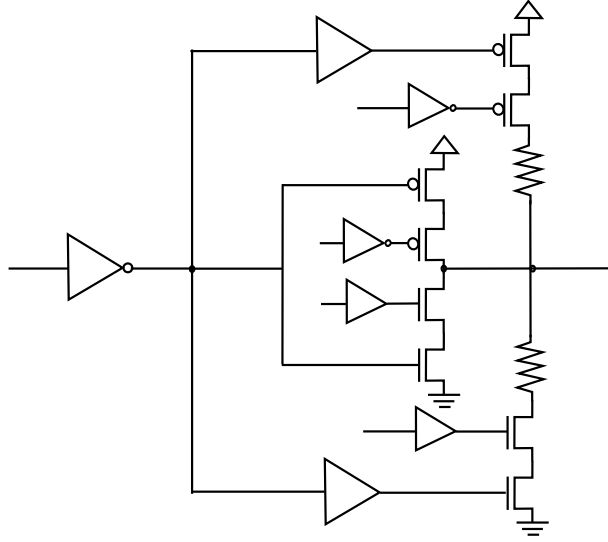


Figure 4.4: Schematic of a voltage mode double inverter tristate driver.

capacitive vs galvanic coupling, signal vs ground electrode and horizontal vs vertical electrode/coupler in Section 2.3 of Chapter 2. The basic architecture of the double inverter tri-state voltage mode driver, designed in 65 nm CMOS technology is shown in Fig. 4.4 and is reported in [100] supervised by the author. The output stage MOSFETs (NMOS and PMOS) have large widths to support 6 mA of current sinking and sourcing. The output driver is simulated for load capacitances 1 pF to 100 pF range as the loading effect due to skin-electrode impedance is not exactly known. It is shown through EM simulations in [61] that if the complex path impedance between the transmitting and receiving node is expressed as a two-port network then input impedance calculated either at the transmitter or receiver side varies with different body positions and distances between them. So the loading effect is a variable quantity. The simulated eye diagram for the double inverter tri-state voltage mode driver with 10 mV supply noise addition for 7.5 ns is shown in Fig. 56 of [100] which gives information about jitter, rise/fall time and inter symbol interference. The vertical eye opening is 1.1 V and horizontal eye opening is 2.5 ns. The timing variation at zero crossing is 0.55 ns, cycle to cycle jitter w.r.t reference clock is 0.87 %, rise time is 1.2 ns while fall time is 1.5 ns.

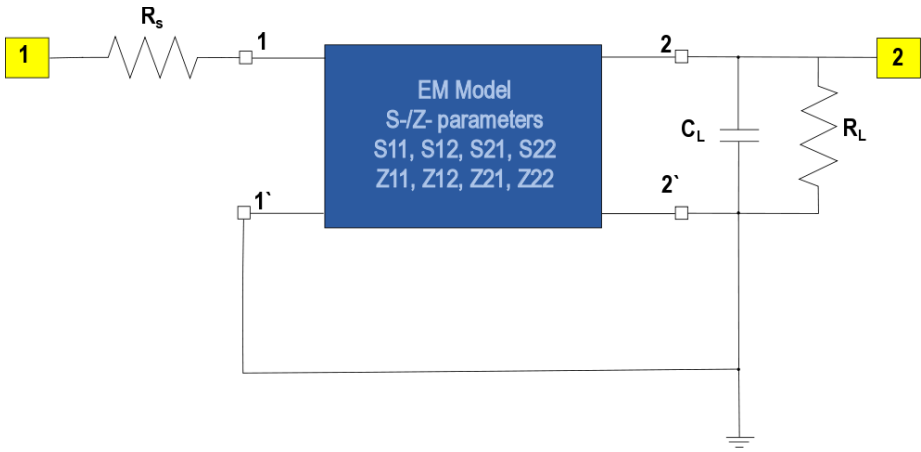


Figure 4.5: EM/circuit co-simulation set-up.

Table 4.1: Electromagnetic models for simulation-setup.

EM Models	Description
A	Skin-Rec arm model with vertical electrodes $[4 \times 4 \times 3] \text{ cm}^3$ at a distance of 50 cm
B	Str4 arm model with vertical electrodes $[4 \times 4 \times 3] \text{ cm}^3$ at a distance of 50 cm
C	Skin-Rec arm model with vertical electrodes $[4 \times 4 \times 1] \text{ cm}^3$ at a distance of 50 cm
D	Str4 arm model with vertical electrodes $[4 \times 4 \times 1] \text{ cm}^3$ at a distance of 50 cm

Table 4.2: Variation of  $R_S$ ,  $C_L$  and  $R_L$ .

Cases	$R_S$ [ $\Omega$ ]	$C_L$ [F]	$R_L$ [ $\Omega$ ]
I	0	0	50
II	0	500f	50
III	0	10p	50
IV	0	50p	50
V	0	0	50
VI	50	0	50
VII	200	0	50
VIII	700	0	50
IX	50	0	0
X	50	0	50
XI	50	0	1k
XII	50	0	10k
XIII	50	0	1M

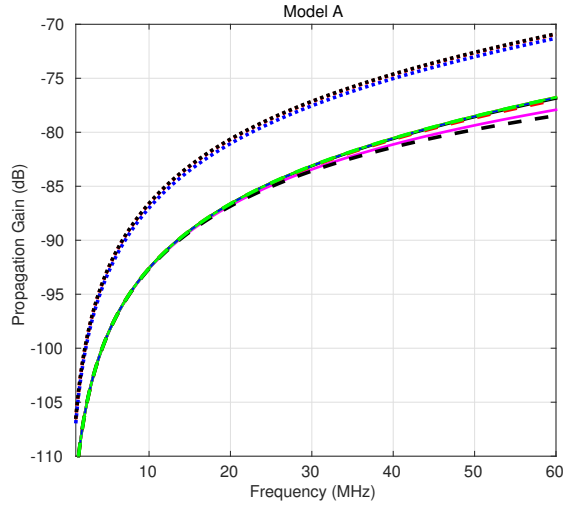


Figure 4.6: EM/circuit co-simulation of Model A; case: I (blue), II (red), III (black), IV (magenta), V (green) [solid], VI (blue), VII (red), VIII (black), IX (magenta), X (green) [dashed], XI (blue), XII (red), XIII (black) [dotted].

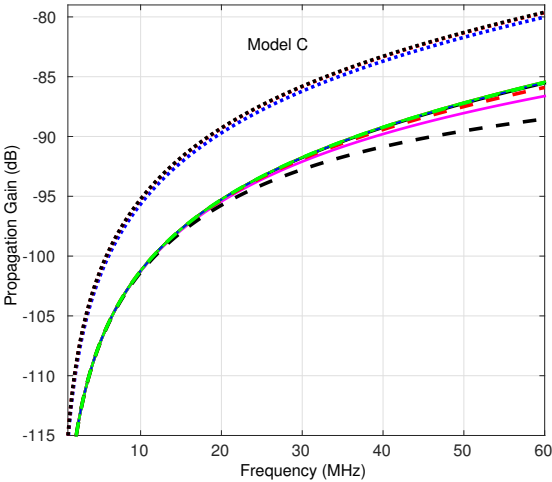


Figure 4.7: EM/circuit co-simulation of Model C; All plots from cases I to XIII have the same colours as Model A.

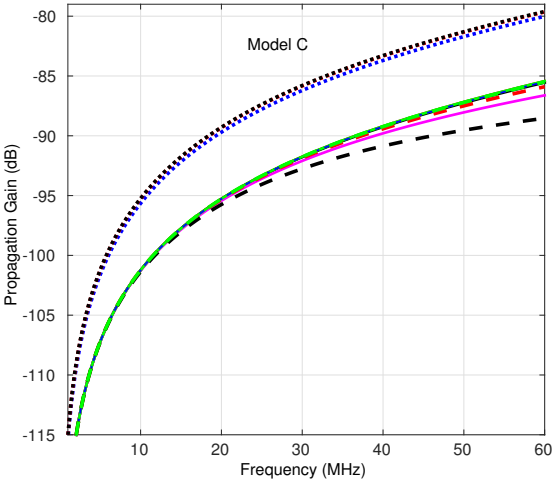


Figure 4.8: EM/circuit co-simulation of Model D; All plots from cases I to XIII have the same colours as Model A.

## 4.5 EM/Circuit Co-simulation to Determine System Specifications

It is difficult to experimentally determine the complex path impedance between transmitter and receiver. Therefore, an alternate simulation strategy has been adapted where the complex path impedance of human body is modeled as a two port network in the form of S-parameters ( $S_{11}$ ,  $S_{12}$ ,  $S_{21}$ ,  $S_{22}$ ) in a standard 3D EM field solver and simulator. These S-parameters vary as a function of transmitter/receiver locations, their relative distances, body positions and electrode configuration/sizes over a wide range of frequencies as presented in [61]. For this purpose the human body is modeled as both, a uniform or a stratified medium to the closest possible measured values of tangent loss,  $\epsilon'$  and  $\epsilon''$  for skin and intermediate dielectric tissue layers. The corresponding S-parameters can be converted in to their equivalent Z-parameters as also discussed in the well known text book of electromagnetics by Pozar [69]. These S or Z parameters could be imported to any circuit simulator where they can be co-simulated with wide range of active or passive circuit elements for standard circuit analysis to help in understanding the system constraints on basic fundamental circuit blocks for defining the system specifications.

The electromagnetic (EM) simulations (S-parameters) of skin-only-rectangle (Sk-Rec) and standard four-layer-stratified (Str4) human-arm models with vertical electrodes of  $[4 \times 4 \times 1]$  and  $[4 \times 4 \times 3]$  cm<sup>3</sup> for a communication distance of 50 cm have been carried out in computer simulation technology (CST) microwave studio (MWS) using 50 ohm discrete-ports and transient solver. The S-parameters of the two port network can be converted to their equivalent Z-parameters in computer simulation technology (CST) microwave studio (MWS) itself for convenience. The Z-parameters ( $Z_{11}$ ,  $Z_{12}$ ,  $Z_{21}$ ,  $Z_{22}$ ) can be imported to Cadence software where EM/circuit co-simulation can be performed. However, the EM/circuit co-simulation is performed in CST Design Studio to check the effect of source resistance ( $R_S$ ), loading capacitance ( $C_L$ ) and loading resistance ( $R_L$ ). The EM/circuit co-simulation setup is illustrated in Fig 4.5.

The description of electromagnetic models is tabulated in Table 4.1. The variation of source resistance ( $R_S$ ), loading capacitance ( $C_L$ ) and loading resistance ( $R_L$ ) is performed for each electromagnetic model as per Table 4.2. The EM/circuit co-simulation is performed for models A, C and D for all the cases to investigate the effect on propagation gain which is ( $|S_{21}|$  [dB]) parameter. The results are shown in Figs. 4.6, 4.7 and 4.8. It shows that the propagation gain improves with the variation of  $R_L$  which is modeled as the input resistance of receiver amplifier.

## 4.6 Summary

The front end amplifier on receiver side and output driver on transmitter side are the most crucial building blocks for capacitive BCC digital baseband

and passband communication. Different performance parameters and design trade-offs for the front end amplifier and tri-state voltage-mode driver in deep submicron CMOS technologies have been discussed. The salient features of digital baseband and passband communication architectures used in the experimental demonstration of capacitive BCC channel are described. The experimental results are discussed in Papers D and E of the thesis. Capacitive electrodes constitute an important part of capacitive BCC transmitter/receiver architecture. The influence of electrode configuration and size in determining the propagation loss for capacitive BCC channel can be found in detail in Papers A, B and C of the thesis. Lastly, it has been shown that the electromagnetic model in the form of S- or Z-parameters as a consequence of proposed variation-aware simulation strategy could be extended to circuit simulators to derive useful system specifications for capacitive BCC transmitter/receiver design.



---

# Summary, Conclusions and Recommendations

## 5.1 Summary and Conclusions

The advent of future generations of connected devices in the realm of wireless sensor network (WSN) and internet-of-things (IoT) demand short range wireless technologies which could meet low data rate and low power consumption requirements for machine-to-machine (M2M) communication in a close vicinity around human body. The devices can communicate with a central hub which can be most likely a personalized mobile phone. Capacitive BCC can serve as an alternate wireless technology which uses human body as a communication channel. The experimental complexity for this mode of communication is to mainly keep the isolation of earth ground during all measurement scenarios which otherwise provides an alternate low impedance return path thus giving rise to an unrealistic path loss. A large number of experiments, performed to measure the propagation loss of a capacitive BCC channel, are found in the literature which fall under the above mentioned category of experimental measurement error/uncertainty. The other factors which cause experimental measurement error/uncertainty are, insufficient cut-off frequency of analog front end, measurements performed on uniform muscle equivalent human phantoms and use of balun or transformers with the earth grounded instruments for the purpose of electrical isolation.

The realistic estimation of the path loss for capacitive BCC channel is investigated by proposing and adapting an alternate strategy for 3D modeling of structures, in the form of uniform or stratified dielectric medium, using their finite conductivity, permittivity or tangent loss profile. The 3D structures are not only limited to human body. The electromagnetic simulations of meshed structures is performed in a commercially available tool. The simulations are performed for communication distances even larger than 50 cm in the frequency range of 1 MHz to 60 MHz for which there is less evidence of measured propagation loss

in the literature. This simulation methodology helps in addressing the above mentioned experimental challenges and comprises the first major part of PhD research work described in Papers A, B and C of the thesis.

In Paper A, the presented efficient full-wave electromagnetic simulation methodology has been evaluated for numerical uncertainties in the form of variations in boundary conditions and number of mesh cells for both horizontal and vertical electrode configurations. Similarly human body dielectric properties in the form of complex permittivity, tangent loss and dielectric thickness is varied for both the uniform skin-only and 4 layer stratified models. The purpose is to evaluate the proposed strategy against realistic variations of human skin and underlying tissue layers electrophysiological properties from person to person due to difference in age, gender, body locations, humidity content and number of cells etc. The propagation loss simulation results are also validated with the measurement results from the literature. The simulation methodology successfully explains the physical phenomenon of complex path loss scenarios due to combined effect of electrode coupler configuration/size, whole human body model, different locations of transmitting/receiving couplers, environmental factors like grounding conditions and metallic/dielectric structures. The proposed simulation strategy helps in categorically extending the Zimmerman generalized capacitive return path theory by showing that the horizontal electrode configuration is more affected by the electrophysiological properties of skin and underlying tissue layers than the capacitive return path. Vertical electrode configuration is, on the other hand, less affected by the underlying tissue variations and they can overcome the limitations of capacitive return path to detect the surface waves from extreme body positions, if the height of the vertical electrode is high enough. The vertical couplers show variations in the propagation loss up to 2 dB while the horizontal couplers show variations from 10 dB to 15 dB in the frequency range of 1 MHz to 60 MHz with communication distances up to 155 cm. The influence of different physical factors on the link-budget requirement for capacitive BCC channel is well investigated as a consequence of the presented simulation methodology. In Paper B, the proposed simulation methodology is compared with Joonsung Bae analytical model which was originally presented for calculating the radiated component of electric field due to surface waves on the surface of damped soil from a vertical dipole type antenna in a paper published in two parts in 1936 and 1937. The efficient full-wave numerical analysis technique reliably estimates the realistic path loss for different body positions, coupler sizes/types, grounding conditions and dielectric mediums which Bae analytical model is not able to explain, although it is computationally more efficient. However, Bae analytical model provides useful direct insight about the factors influencing the signal propagation due to vertical electrodes configuration by simplified mathematical expressions. The proposed simulation model does not provide simplified mathematical expressions. In Paper C, capacitive BCC channel has been modeled as a 2-port complex path impedance  $[Z]$  whose  $[Z]$  parameters ( $Z_{11}$ ,  $Z_{12}$ ,  $Z_{21}$  and  $Z_{22}$ ) have been estimated using systematic

numerical simulation methodology proposed in Paper A. The equivalent input impedance  $Z_{in}$  at the transmitter side or equivalent output impedance  $Z_{out}$  on the receiver side is expressed in terms of Z-parameters which varies as a function of different body positions over the given frequency range of 1 MHz to 60 MHz. If either  $Z_{in}$  or  $Z_{out}$  are conjugate matched to either  $Z_s$  or  $Z_L$ , then maximum power transfer condition is satisfied. It is found that for maximum power transfer resistive matching below 1000  $\Omega$  and inductive matching between 0.5  $\mu\text{H}$  to 5  $\mu\text{H}$  on any side of the two ports is required for given body positions over given frequency range. Another consequence of expressing capacitive BCC attenuation channel in terms of Z-parameters or S-parameters is that these parameters can be readily integrated with the standard circuit design simulation tools and help in defining the system specifications for designing BCC transceivers. As an example, the effect of varying source resistance ( $R_s$ ), loading capacitance ( $C_L$ ) and loading resistance ( $R_L$ ) is performed for skin-only rectangle (Skin-Rec) and 4-layer stratified (Str4) human-arm models with vertical electrodes of two different dimensions for a communication distance of 50 cm. The EM/circuit co-simulation is performed which investigates their effect on propagation gain ( $|S_{21}|$  [dB]) as plotted in Section 4.5. The chapters 2 and 3 provide necessary background for the understanding of Papers A, B and C.

The second part of the research work, reported in Papers D and E, deals with the experimental demonstration of digital baseband and passband (resonance mode) communication architectures using discrete electronic components in the context of IoT application. The experimental work discusses a number of physical factors which directly influence the capacitive BCC channel like the effect of ground plane on human body, effect of partially grounded conditions on digital baseband signaling architecture, phenomenon of virtual electrodes formation, effect of electrode configuration/size on packet transmission, effect of different body positions on packet transmission, effect of output driver configuration and current sourcing/sinking on signal transmission, effect of using grounded instrument on packet transmission for battery operated transmitter and receiver and effect of using high order bandpass filter in the receiver, etc. The results discussed in Papers D and E regarding packet error rate under different electrode configurations and body positions for different communication architectures ensure that the experimental setup has been designed to completely isolate the earth ground during all measurements for battery operated transmitter and receiver. The condition of earth ground isolation has been violated in most of the experiments presented in the literature which all together changes the focus of the problem. The architectures chosen for experimental measurements are not necessarily the best ones but they are suitable for low data rate applications between 1 kbps to 100 kbps specially in the application scenario of reading digital information stored in the micro-controller memory and transmitting it though human body communication channel to BCC receiver attached to a portable/mobile platform. The purpose of experimental demonstration is not the optimization of power consumption as it is not possible to optimize the

power in a design made of discrete electronic components which uses a general purpose FPGA/micro-controller for digital processing. A part of the design effort was to focus on an intentional dissimilar design to take the advantage of low power consumption. Dissimilar design means that the transmitter and receiver are separated from each other so that the transmitter along with the digital memory could essentially be implemented in a single low power consumption micro-controller taking advantage of its powerful power management in order to increase the battery life time. This concept has been demonstrated in Paper D with screen printed electrodes as well and the possibility of low power capacitive BCC transmitter implementation in the emerging printed technologies like organic thin film transistors have also been discussed with their pros and cons. The communication architectures give useful insight about the most essential analog building blocks for resilience against noise. The choice of simple digital baseband architecture, which uses only cascaded amplifiers and schmitt trigger helps in emphasizing the role of analog filtering in the receiver AFE, if the loading conditions have properly been taken care.

The third part of the research deals with the integrated circuit design of most essential analog building blocks in the capacitive BCC transmitter/receiver in deep submicron CMOS technologies like ST 65 nm and 40 nm. The most essential block for the successful transmission is identified as the output driver stage for transmitter and front end low noise amplifier for receiver. The design of two different OTA topologies, split-length current mirror load [101] and current shunt current mirror OTA [102] as front end low noise amplifier have been discussed highlighting their most essential parameters and their conflicting trade-offs for the design of capacitive BCC receiver. The desirable characteristics are high CMRR/PSRR to avoid common mode noise from coupling with receiver circuit, low rms integrated input referred noise with low noise bandwidth to detect signal which is four orders of magnitude smaller than the maximum signal, high cut-off frequency for 0.1 dB flat bandwidth but low unity gain frequency to reduce noise bandwidth and low power consumption for which number of closed loop cascaded amplifier stages are replaced by single open loop high gain stage and internal frequency compensation capacitor is also avoided. The design of tri-state voltage mode output driver is discussed in Section 4.4.2 of the thesis for current sinking/sourcing capability, varying largely the capacitive loading effects, cycle to cycle jitter w.r.t clock, timing variations at zero crossing and rise/fall times etc in CMOS 65nm technology. The voltage mode driver may not be a suitable choice w.r.t power consumption as it consumes around 7.5 mW of power for peak current sourcing/sinking of 6 mA.

The goal of the thesis was to understand the physical factors, directly influencing the human body as a communication channel, both experimentally and through system level simulations. For this purpose, a top-down system design methodology is proposed which allows the EM simulations for the variation and physical phenomenon-aware design of capacitive BCC channel along with the circuit parameters to define system specifications for transmitter/receiver design.

The challenges of capacitive BCC channel are unique in the sense that it is a highly attenuated channel with better conducting properties than air at low frequencies. The horizontal coplanar electrode configuration may experience the difference in ground references when the transmitter and receiver ground electrodes are touching the human body while the vertical electrodes present a floating ground condition for the circuit. The influence of body positions and transmitter/receiver locations on human body is also evident from the simulations and experiments. If the physical factors which influence the capacitive BCC channel are known prior to the circuit design and incorporated with the circuit simulators through a suitable system design methodology which allows the co-simulation of these physical factors then it is possible to design exclusive circuit design to meet the capacitive BCC channel characteristics under all possible communication scenarios. This PhD dissertation is also an attempt to propose such a system design methodology.

## 5.2 Recommendations

The proposed strategy uses full-wave EM simulations in [26] to realistically estimate the propagation loss characteristics of capacitive BCC channel in complex scenarios due to the combined interaction of coupler, human body and environment. It also allows to estimate the complex path impedance including the loading effects of uncertain skin-electrode impedance which defines the bounds on the impedance matching requirements for the sake of maximum power transfer. This simulation methodology can be directly integrated with the circuit simulators to take the effects of capacitive BCC channel in the design phase.

In the literature, mostly quasi-electrostatic condition is assumed to model and analyze the capacitive BCC channel even upto a few MHz region to keep the modeling and computations simple. Some examples are [6], [46], [47], [59], and [60]. There is no work in the literature which compares both the quasi-electrostatic and full-wave electromagnetic models to determine the propagation loss for capacitive BCC channel with the measurement results in the controversial few MHz region. Further more, the magnetic component can be computed separately in quasi-magnetostatic field solvers in a few MHz region to compare with the magnetic field component determined by the full-wave EM simulations. The magnetic field components may closely match in a few MHz region. The challenge is that equivalent lumped electrical model could be derived directly with quasi-electrostatic and quasi-magnetostatic models but full-wave gives output in the form of S-parameters. So some intermediate strategy is needed to be devised for comparison. The detailed human body voxel models could be used for the horizontal couplers, to see the extent of variations and simplified assumptions which could be adapted to reduce the computation time. These analysis will contribute significantly towards further confirming the authenticity of the proposed simulation strategy in [26], [103] and [61].



---

## References

- [1] T. G. Zimmerman, "Personal area networks (pan): Near-field intra-body communication," Ph.D. dissertation, Citeseer, 1995.
- [2] —, "Personal area networks: Near-field intrabody communication," *IBM Systems Journal*, vol. 35, no. 3, pp. 609 – 617, 1996.
- [3] M. Fukumoto and Y. Tonomura, "Body coupled fingerring: wireless wearable keyboard," *Proceedings of the SIGCHI conference on Human factors in computing systems - CHI97*, 1997.
- [4] T. Handa, S. Shoji, S. Ike, S. Takeda, and T. Sekiguchi, "A very low-power consumption wireless ECG monitoring system using body as a signal transmission medium," *Proceedings of International Solid State Sensors and Actuators Conference (Transducers 1997)*, 1997.
- [5] K. Hachisuka, A. Nakata, T. Takeda, Y. Terauchi, K. Shiba, K. Sasaki, H. Hosaka, and K. Ito, "Development and performance analysis of an intra-body communication device," in *Proc. TRANSDUCERS, Solid-State Sensors, Actuators and Microsystems, 12th Int. Conf.*, vol. 2, 2003, pp. 1722 – 1725.
- [6] K. Hachisuka, Y. Terauchi, Y. Kishi, K. Sasaki, T. Hirota, H. Hosaka, K. Fujii, M. Takahashi, and K. Ito, "Simplified circuit modeling and fabrication of intrabody communication devices," *Sensors and Actuators A: Physical*, vol. 130-131, pp. 322–330, Aug 2006.
- [7] K. Fujii, K. Ito, and S. Tajima, "Signal propagation of wearable computing using human body as transmission channel," *Proceedings of the International Symposium on Antennas and Propagation ISAP-02*, pp. 512 – 515, 2002.
- [8] —, "A study on the receiving signal level in relation with the location of electrodes for wearable devices using human body as a transmission channel," in *Antennas and Propagation Society International Symposium, 2003. IEEE*, vol. 3, 2003, pp. 1071 – 1074.

- [9] K. Fujii, M. Takahashi, K. Ito, and N. Inagaki, "Study on the electric field distributions around whole body model with a wearable device using the human body as a transmission channel," in *Antennas and Propagation, 2006. EuCAP 2006. First European Conference on*. IEEE, 2006, pp. 1–4.
- [10] K. Fujii, M. Takahashi, and K. Ito, "Electric field distributions of wearable devices using the human body as a transmission channel," *IEEE Trans. Antennas Propag.*, vol. 55, no. 7, pp. 2080–2087, 2007.
- [11] T. Yanagida, "Human body communication system and communication device," Feb 2010. [Online]. Available: <http://www.google.com/patents/US7664476>
- [12] J. Ruiz and S. Shimamoto, "Experimental evaluation of body channel response and digital modulation schemes for intra-body communications," *2006 IEEE International Conference on Communications*, 2006.
- [13] J. Ruiz, J. Xu, and S. Shimamoto, "Propagation characteristics of intra-body communications for body area networks," *CCNC 2006. 2006 3rd IEEE Consumer Communications and Networking Conference*, 2006., 2006.
- [14] N. Cho, J. Yoo, S.-J. Song, J. Lee, S. Jeon, and H.-J. Yoo, "The human body characteristics as a signal transmission medium for intrabody communication," *IEEE Trans. Microw. Theory Techn.*, vol. 55, no. 5, pp. 1080 – 1086, 2007.
- [15] T. C. W. Schenk, N. S. Mazloun, L. Tan, and P. Rutten, "Experimental characterization of the body-coupled communications channel," in *Wireless Communication Systems. 2008. ISWCS '08. IEEE International Symposium on*, 2008, pp. 234–239.
- [16] B. Gyselinckx, C. Van Hoof, J. Ryckaert, R. Yazicioglu, P. Fiorini, and V. Leonov, "Human++: autonomous wireless sensors for body area networks," *Proceedings of the IEEE 2005 Custom Integrated Circuits Conference*, 2005., 2005.
- [17] S. Movassaghi, M. Abolhasan, J. Lipman, D. Smith, and A. Jamalipour, "Wireless body area networks: A survey," *IEEE Commun. Surv. Tutorials*, vol. 16, no. 3, pp. 1658 – 1686, 2014.
- [18] D. D. He, E. S. Winokur, and C. G. Sodini, "A continuous, wearable, and wireless heart monitor using head ballistocardiogram (bcg) and head electrocardiogram (ECG)," *2011 Annual International Conference of the IEEE Engineering in Medicine and Biology Society*, Aug 2011.
- [19] —, "An ear-worn continuous ballistocardiogram (bcg) sensor for cardiovascular monitoring," *2012 Annual International Conference of the IEEE Engineering in Medicine and Biology Society*, Aug 2012.

- [20] *IEEE Standard for Local and metropolitan area networks Part 15.6: Wireless Body Area Networks*, LAN/MAN Standards Committee of the IEEE Computer Society Std. IEEE 802.15.6, February 2012.
- [21] A. P. Fernández, “Towards the tangible hyperlink,” in *The Seventh International Conference on Advances in Computer-Human Interactions*. IARIA, March 2014, pp. 17 – 20.
- [22] S.-J. Song, N. Cho, S. Kim, J. Yoo, and H.-J. Yoo, “A 2Mb/s wideband pulse transceiver with direct-coupled interface for human body communications,” *2006 IEEE International Solid State Circuits Conference - Digest of Technical Papers*, 2006.
- [23] S.-J. Song, N. Cho, S. Kim, J. Yoo, S. Choi, and H.-J. Yoo, “A 0.9V 2.6mW body-coupled scalable PHY transceiver for body sensor applications,” *2007 IEEE International Solid-State Circuits Conference. Digest of Technical Papers*, Feb 2007.
- [24] N. Cho, J. Lee, L. Yan, J. Bae, S. Kim, and H.-J. Yoo, “A 60kb/s-to-10Mb/s 0.37nJ/b adaptive-frequency-hopping transceiver for body-area network,” *2008 IEEE International Solid-State Circuits Conference - Digest of Technical Papers*, Feb 2008.
- [25] A. Fazzi, S. Ouzounov, and J. van den Homberg, “A 2.75 mW wideband correlation-based transceiver for body-coupled communication,” in *Solid-State Circuits Conference - Digest of Technical Papers, 2009. ISSCC 2009. IEEE International*, 2009, pp. 204–205.
- [26] M. Irfan Kazim, M. Imran Kazim, and J. J. Wikner, “An Efficient Full-Wave Electromagnetic Analysis for Capacitive Body-Coupled Communication,” *International Journal of Antennas and Propagation*, vol. 2015, no. 245621, May 2015.
- [27] H. Baldus, S. Corroy, A. Fazzi, K. Klabunde, and T. Schenk, “Human-centric connectivity enabled by body-coupled communications,” *IEEE Commun. Mag.*, vol. 47, no. 6, pp. 172 – 178, 2009.
- [28] N. S. Mazloum, “Body-coupled communications: Experimental characterization, channel modeling and physical layer design,” Master’s thesis, Chalmers University of Technology Philips Research: Department of Signals and Systems Distributed Sensor Systems, December 2008.
- [29] J. A. Ruiz and S. Shimamoto, “Experimental evaluation of body channel response and digital modulation schemes for intra-body communications,” in *Proc. IEEE Int. Conf. Communications ICC '06*, vol. 1, 2006, pp. 349 – 354.

- [30] R. Xu, H. Zhu, and J. Yuan, "Electric-field intrabody communication channel modeling with finite-element method," *Biomedical Engineering, IEEE Transactions on*, vol. 58, no. 3, pp. 705–712, 2011.
- [31] J. Sakai, L.-S. Wu, H.-C. Sun, and Y.-X. Guo, "Baluns effect on the measurement of transmission characteristics for intrabody communication channel," *2013 IEEE MTT-S International Microwave Workshop Series on RF and Wireless Technologies for Biomedical and Healthcare Applications (IMWS-BIO)*, Dec 2013.
- [32] H. Z. Ruoyu Xu and J. Yuan, "Circuit-coupled FEM analysis of the electric-field type intra-body communication channel," in *Biomedical Circuits and Systems Conference, 2009. BioCAS 2009. IEEE*, 2009, pp. 221–224.
- [33] H. Zhu, R. Xu, and J. Yuan, "High speed intra-body communication for personal health care," *2009 Annual International Conference of the IEEE Engineering in Medicine and Biology Society*, Sep 2009.
- [34] M. Wegmueller, S. Huclova, J. Froehlich, M. Oberle, N. Felber, N. Kuster, and W. Fichtner, "Galvanic coupling enabling wireless implant communications," *IEEE Transactions on Instrumentation and Measurement*, vol. 58, no. 8, pp. 2618–2625, Aug 2009.
- [35] T. Yamamoto and Y. Yamamoto, "Electrical properties of the epidermal stratum corneum," *Medical & Biological Engineering*, vol. 14, no. 2, pp. 151–158, Mar 1976.
- [36] Z. Ya-Xian, T. Suetake, and H. Tagami, "Number of cell layers of the stratum corneum in normal skin - relationship to the anatomical location on the body, age, sex and physical parameters," *Archives of Dermatological Research*, vol. 291, no. 10, pp. 555 – 559, Nov 1999.
- [37] J. Rosell, J. Colominas, P. Riu, R. Pallas-Areny, and J. Webster, "Skin impedance from 1 Hz to 1 MHz," *IEEE Trans. Biomed. Eng.*, vol. 35, no. 8, pp. 649–651, 1988.
- [38] J. D. Jackson, *Classical Electrodynamics*, 3rd ed. Wiley, NewYork, 1999.
- [39] J. Larsson, "Electromagnetics from a quasistatic perspective," *American Journal of Physics*, vol. 75, no. 3, pp. 230 – 239, 2007.
- [40] M. Cartier and K. U. Sivaprasad, "A measurement based comparison of full-wave and quasi-static methods for baseband modeling of plated through hole structures to 20GHz," *2007 Proceedings 57th Electronic Components and Technology Conference*, 2007.
- [41] M. S. Wegmüller *et al.*, "Intra-body communication for biomedical sensor networks," Ph.D. dissertation, Diss., Eidgenössische Technische Hochschule ETH Zürich, Nr. 17323, 2007, 2007.

- [42] R. Xu, W. C. Ng, H. Zhu, H. Shan, and J. Yuan, "Equation environment coupling and interference on the electric-field intrabody communication channel," *IEEE Trans. Biomed. Eng.*, vol. 59, no. 7, pp. 2051–2059, Jul 2012.
- [43] K. Fujii and K. Ito, "Evaluation of the received signal level in relation to the size and carrier frequencies of the wearable device using human body as a transmission channel," *IEEE Antennas and Propagation Society Symposium, 2004.*, 2004.
- [44] K. Fujii, D. Ishide, M. Takahashi, and K. Ito, "Electric field distributions generated by a wearable device using simplified whole human body models," *Information and Media Technologies*, vol. 4, no. 2, pp. 647 – 654, 2009.
- [45] J. Hwang, C. H. Hyoun, J. B. Sung, J. K. Kim, D. G. Park, and S. W. Kang, "Em simulation and analysis on the ground electrode of human body communication," in *Microwave Conference, 2006. 36th European*, 2006, pp. 1122 – 1123.
- [46] N. Haga, K. Saito, M. Takahashi, and K. Ito, "Proper derivation of equivalent-circuit expressions of intra-body communication channels using quasi-static field," *IEICE Transactions on Communications*, vol. E95.B, no. 1, pp. 51–59, 2012.
- [47] —, "Equivalent circuit of intrabody communication channels inducing conduction currents inside the human body," *Antennas and Propagation, IEEE Transactions on*, vol. 61, no. 5, pp. 2807–2816, May 2013.
- [48] W. Dally and J. Poulton, *Digital Systems Engineering*. Cambridge University Press, 1998. [Online]. Available: [https://books.google.se/books?id=oDWRAxCU-\\_g8C](https://books.google.se/books?id=oDWRAxCU-_g8C)
- [49] C. R. Paul, *Introduction to Electromagnetic Compatibility*, 2nd ed. John Wiley & Sons, 2008.
- [50] C. Aliau-Bonet and R. Pallas-Areny, "On the effect of body capacitance to ground in tetrapolar bioimpedance measurements," *IEEE Trans. Biomed. Eng.*, vol. 59, no. 12, pp. 3405–3411, Dec 2012.
- [51] R. Serrano, M. Gasulla, O. Casas, and R. Pallas-Areny, "Power line interference in ambulatory biopotential measurements," *Proceedings of the 25th Annual International Conference of the IEEE Engineering in Medicine and Biology Society (IEEE Cat. No.03CH37439)*, 2003.
- [52] M. Haberman, A. Cassino, and E. Spinelli, "Estimation of stray coupling capacitances in biopotential measurements," *Medical & Biological Engineering & Computing*, vol. 49, no. 9, pp. 1067–1071, Jul 2011.

- [53] C. Assambo, A. Baba, R. Dozio, and M. Burke, “Determination of the parameters of the skin-electrode impedance model for ecg measurement,” in *Proceedings of the 6th WSEAS international conference on electronics, hardware, wireless and optical communications, Corfu Island, Greece, 2007*, pp. 90 – 95.
- [54] M. R. Neuman, *Medical Instrumentation Application and Design*. John Wiley & Sons, 2009, ch. Biopotential Electrodes.
- [55] C. R. Paul, *Introduction to Electromagnetic Compatibility (Wiley Series in Microwave and Optical Engineering)*. Wiley-Interscience, 2006.
- [56] S.-J. Song, N. Cho, S. Kim, and H.-J. Yoo, “A 4.8 mW 10 Mb/s wideband signaling receiver analog front-end for human body communications,” in *Solid-State Circuits Conference, 2006. ESSCIRC 2006. Proceedings of the 32nd European*, 2006, pp. 488–491.
- [57] S.-J. Song, N. Cho, and H.-J. Yoo, “A 0.2 mw 2 mb/s digital transceiver based on wideband signaling for human body communications,” *IEEE J. Solid-State Circuits*, vol. 42, no. 9, pp. 2021–2033, 2007.
- [58] J. Bae, H. Cho, K. Song, H. Lee, and H.-J. Yoo, “The signal transmission mechanism on the surface of human body for body channel communication,” *IEEE J. MTT*, vol. 60, no. 3, pp. 582 – 593, 2012.
- [59] M. S. Wegmueller, A. Kuhn, J. Froehlich, M. Oberle, N. Felber, N. Kuster, and W. Fichtner, “An attempt to model the human body as a communication channel,” *IEEE Trans. Biomed. Eng.*, vol. 54, no. 10, pp. 1851 – 1857, 2007.
- [60] K. Fujii and Y. Okumura, “Effect of earth ground and environment on body-centric communications in the MHz band,” *International Journal of Antennas and Propagation*, vol. 2012, pp. 1–10, 2012.
- [61] M. Irfan Kazim, M. Imran Kazim, and J. J. Wikner, “Complex path impedance estimation and matching requirements for body-coupled communication,” in *2015 European Conference on Circuit Theory and Design (ECCTD)*. Institute of Electrical & Electronics Engineers (IEEE), August 2015.
- [62] —, “Complex path impedance estimation and matching requirements for body-coupled communication,” in *2015 European Conference on Circuit Theory and Design (ECCTD)*. Institute of Electrical & Electronics Engineers (IEEE), August 2015.
- [63] H. Nishiyama and M. Nakamura, “Form and capacitance of parallel-plate capacitors,” *IEEE Trans. Comp., Packag., Manufact. Technol. A*, vol. 17, no. 3, pp. 477–484, 1994.

- [64] K. A. Norton, "The propagation of radio waves over the surface of the earth and in the upper atmosphere," *Proc. IRE*, vol. 24, no. 10, pp. 1367–1387, Oct 1936.
- [65] —, "The propagation of radio waves over the surface of the earth and in the upper atmosphere," *Proc. IRE*, vol. 25, no. 9, pp. 1203–1236, Sep 1937.
- [66] S. Gabriel, R. Lau, and C. Gabriel, "The dielectric properties of biological tissues: III. parametric models for the dielectric spectrum of tissues," *Physics in medicine and biology*, vol. 41, no. 11, p. 2271, 1996.
- [67] W. L. Stutzman and G. A. Thiele, *Antenna theory and design*, 2nd ed. Chichester: Wiley, 1998.
- [68] *HF Design and Analysis - CST Microwave Studio - Advanced Topics Version 4*.
- [69] D. Pozar, *Microwave Engineering*. Wiley, 2004.
- [70] C. Furse, D. A. Christensen, and C. H. Durney, *Basic introduction to bioelectromagnetics*. CRC press, 2009.
- [71] IFAC-CNR. (1997) An internet resource for the calculation of the dielectric properties of body tissues in the frequency range 10 Hz - 100 GHz. IFAC-CNR. IFAC-CNR, Florence (Italy). [Online]. Available: <http://niremf.ifac.cnr.it/tissprop/>
- [72] C. Gabriel, S. Gabriel, and E. Corthout, "The dielectric properties of biological tissues: I. literature survey," *Physics in medicine and biology*, vol. 41, no. 11, p. 2231, 1996.
- [73] S. Gabriel, R. Lau, and C. Gabriel, "The dielectric properties of biological tissues: II. measurements in the frequency range 10 Hz to 20 Ghz," *Physics in medicine and biology*, vol. 41, no. 11, p. 2251, 1996.
- [74] L. Rattfält, F. Björefors, D. Nilsson, X. Wang, P. Norberg, and P. Ask, "Properties of screen printed electrocardiography smartware electrodes investigated in an electro-chemical cell," *BioMedical Engineering OnLine*, vol. 12, no. 1, p. 64, 2013.
- [75] T. C. Ferree, P. Luu, G. S. Russell, and D. M. Tucker, "Scalp electrode impedance, infection risk, and EEG data quality," *Clinical Neurophysiology*, vol. 112, no. 3, pp. 536–544, Mar 2001.
- [76] J. C. Huhta and J. G. Webster, "60-Hz interference in electrocardiography," *IEEE Trans. Biomed. Eng.*, vol. BME-20, no. 2, pp. 91–101, Mar 1973.

- [77] P. Lepola, S. Myllymaa, J. Toyras, E. Mervaala, R. Lappalainen, and K. Myllymaa, "Shielded design of screen-printed EEG electrode set reduces interference pick-up," *IEEE Sensors Journal*, vol. 14, no. 8, pp. 2692 – 2697, Aug 2014.
- [78] N. Cho, L. Yan, J. Bae, and H.-J. Yoo, "A 60 kb/s–10 mb/s adaptive frequency hopping transceiver for interference-resilient body channel communication," *IEEE J. Solid-State Circuits*, vol. 44, no. 3, pp. 708 – 717, 2009.
- [79] N. Cho, J. Bae, S. Kim, and H.-J. Yoo, "A 10.8mw body-channel-communication/mics dual-band transceiver for a unified body-sensor-network controller," in *Proc. IEEE Int. Solid-State Circuits Conf. - Digest of Technical Papers ISSCC 2009*, 2009, pp. 424 – 425.
- [80] Y.-T. Lin, Y.-S. Lin, C.-H. Chen, H.-C. Chen, Y.-C. Yang, and S.-S. Lu, "A 0.5 v biomedical system-on-a-chip for intrabody communication system," *IEEE Trans. Ind. Electron.*, vol. 58, no. 2, pp. 690 – 699, 2011.
- [81] J. Bae, K. Song, H. Lee, H. Cho, and H.-J. Yoo, "A 0.24-nj/b wireless body-area-network transceiver with scalable double-fsk modulation," *IEEE J. Solid-State Circuits*, vol. 47, no. 1, pp. 310 – 322, 2012.
- [82] D. Joonsung Bae, K. Song, H. Lee, H. Cho, and H.-J. Yoo, "A low-energy crystal-less double-fsk sensor node transceiver for wireless body-area network," *IEEE J. Solid-State Circuits*, vol. 47, no. 11, pp. 2678–2692, 2012. [Online]. Available: <http://ieeexplore.ieee.org/stamp/stamp.jsp?arnumber=6298034>
- [83] P. Harikumar, M. I. Kazim, and J. J. Wikner, "An analog receiver front-end for capacitive body-coupled communication," in *NORCHIP, 2012*. IEEE, 2012, pp. 1 – 4.
- [84] M. Irfan Kazim and J. J. Wikner, "Design of a sub-mw front-end amplifier for capacitive bcc receiver in 65 nm cmos." Ibcas, 13th International Bhurban conference on Applied Sciences and Technology, January 2016.
- [85] W. M. C. Sansen, *Analog Design Essentials*. Springer, 2006.
- [86] "Ieee standard for safety levels with respect to human exposure to radio frequency electromagnetic fields, 3 khz to 300 ghz," *IEEE Std C95.1-2005 (Revision of IEEE Std C95.1-1991)*, pp. 1 – 238, April 2006.
- [87] "Guidelines for limiting exposure to time-varying electric, magnetic, and electromagnetic fields (up to 300 ghz). international commission on non-ionizing radiation protection." *Health Phys.*, vol. 74, no. 4, pp. 494 – 522, Apr 1998.

- [88] G. S. Anderson and C. G. Sodini, "Body coupled communication: The channel and implantable sensors," *2013 IEEE International Conference on Body Sensor Networks*, May 2013.
- [89] E. Spinelli and M. Haberman, "Insulating electrodes: a review on biopotential front ends for dielectric skin electrode interfaces," *Physiological Measurement*, vol. 31, no. 10, pp. 183–198, Sep 2010.
- [90] J. H. Nagel, *The Biomedical Engineering Handbook*, 2nd ed. CRC press LLC, 2000, ch. Biopotential Amplifiers.
- [91] M. Burke and D. Gleeson, "A micropower dry-electrode ECG preamplifier," *IEEE Trans. Biomed. Eng.*, vol. 47, no. 2, pp. 155–162, 2000.
- [92] E. McAdams, *Bio-Medical CMOS ICs*. Springer, 2011, ch. Biomedical Electrodes For Biopotential Monitoring and Electrostimulation, pp. 31–124.
- [93] H. Yoo and C. van Hoof, *Bio-Medical CMOS ICs*, ser. Integrated Circuits and Systems. Springer, 2011.
- [94] R. Pallas Areny and J. Webster, "AC instrumentation amplifier for bioimpedance measurements," *IEEE Trans. Biomed. Eng.*, vol. 40, no. 8, pp. 830 – 833, 1993.
- [95] A. Chandrakasan, S. Sheng, and R. Brodersen, "Low-power CMOS digital design," *IEEE Journal of Solid-State Circuits*, vol. 27, no. 4, pp. 473–484, Apr 1992. [Online]. Available: <http://dx.doi.org/10.1109/4.126534>
- [96] D. Liu and C. Svensson, "Trading speed for low power by choice of supply and threshold voltages," *IEEE Journal of Solid-State Circuits*, vol. 28, no. 1, pp. 10–17, 1993. [Online]. Available: <http://dx.doi.org/10.1109/4.179198>
- [97] C. Svensson, "Towards power centric analog design," *IEEE Circuits and Systems Magazine*, vol. 15, no. 3, pp. 44–51, 2015. [Online]. Available: <http://dx.doi.org/10.1109/MCAS.2015.2450671>
- [98] L. Yao, M. Steyaert, and W. Sansen, "A 1-V 140  $\mu$ W 88 dB audio sigma-delta modulator in 90-nm CMOS," *IEEE Journal of Solid-State Circuits*, vol. 39, no. 11, pp. 1809–1818, Nov 2004.
- [99] A. M. Van Rijn, A. Peper, and C. Grimbergen, "High-quality recording of bioelectric events," *Medical and Biological Engineering and Computing*, vol. 28, no. 5, pp. 389 – 397, 1990.
- [100] A. Korishe, "A driver circuit for body-coupled communication," Master's thesis, Linköping University, Electronics System, 2013.

- [101] V. Saxena and R. J. Baker, "Compensation of CMOS op-amps using split-length transistors," in *Proc. IEEE Int Midwest Symp. Circuits Syst. (MWSCAS)*, Aug. 2008, pp. 109–112.
- [102] T.-H. Lin, C.-K. Wu, and M.-C. Tsai, "A 0.8 V 0.25 mW current-mirror OTA with 160 MHz GBW in 0.18- $\mu\text{m}$  CMOS," *IEEE Trans. Circuits Syst. II*, vol. 54, no. 2, pp. 131–135, Feb 2007.
- [103] M. I. Kazim, M. I. Kazim, and J. J. Wikner, "Realistic path loss estimation for capacitive body-coupled communication," *2015 European Conference on Circuit Theory and Design (ECCTD)*, Aug 2015. [Online]. Available: <http://dx.doi.org/10.1109/ECCTD.2015.7300105>

## Part II

# Publications



# Publications

The articles associated with this thesis have been removed for copyright reasons. For more details about these see:

<http://urn.kb.se/resolve?urn=urn:nbn:se:liu:diva-122840>

Recent Dissertations  
Division of Integrated Circuits and Systems,  
Department of Electrical Engineering (ISY),  
Linköping University, Sweden

Ameya Bhide, *Design of High-Speed Time-Interleaved Delta-Sigma D/A Converters*, Linköping Studies in Science and Technology, Diss., No. 1688, 2015.

Nadeem Afzal, *Complexity and Power Reduction in Digital Delta-Sigma Modulators*, Linköping Studies in Science and Technology, Diss., No. 1640, 2015.

Niklas U Andersson, *Design of Integrated Building Blocks for the Digital/Analog Interface*, Linköping Studies in Science and Technology, Diss., No. 1638, 2015.

Fahad Qazi, *Selected Applications of Switched Capacitor Circuits: RF N-Path Filters and  $\Sigma \Delta$  Modulators*, Linköping Studies in Science and Technology, Diss., No. 1627, 2015.

Amin Ojani, *Analysis and Design of DLL-Based Frequency Synthesizers for Ultra-Wideband Communication*, Linköping Studies in Science and Technology, Diss., No. 1618, 2014.

Dai Zhang, *Ultra-Low-Power Analog-to-Digital Converters for Medical Applications*, Linköping Studies in Science and Technology, Diss., No. 1611, 2014.

Ali Fazli Yeknami, *Low-Power Delta-Sigma Modulators for Medical Applications*, Linköping Studies in Science and Technology, Diss., No. 1563, 2014.